PRAGUE GEOTECHNICAL DAYS 2015

Resumé

Landslides – Role of Geology and Geotechnics

23TH PRAGUE GEOTECHNICAL LECTURE

Geological approach to landslide evaluation

Jan Novotný[1, 2]
[1)] ARCADIS CZ a.s.
[2)] Institute of Hydrogeology, Engineering Geology and Applied Geophysics,
Faculty of Science, Charles University in Prague, Czech Republic

Extended abstract

The purpose of this presentation is to emphasize the importance of geological understanding in the evaluation of landslides. Only some aspects of this generally very broad topic are discussed, such as the relationship between geomorphology and geology in the evaluation of landslides, the influence of hydrogeological conditions and of soil and rock structure on slope stability. The geological approach in evaluation of landslides was put into context with respect to the generation and use of engineering models in the sense of IAEG commission 25 recommendations (Parry et al 2014) using the working hypothesis that similar landslides in similar materials are caused by similar processes under similar conditions (Cruden & Lan 2014). Cases where a generally accepted geotechnical (analytical, numerical) model is not consistent with the engineering geological model are discussed. The examples selected are cases personally investigated by the author and therefore better known to him than examples from literature.

Two examples from the presentation are selected to be briefly presented here in this extended abstract. The example of the Devechi landslide, Azerbaijan shows the mutual relationship of the geology and geomorphology of the slope and the causes of the landslide. On the contrary, the example of the Březno landslide, Czech Republic shows that even in "geotechnically homogeneous" rocks such as Cretaceous mudstones, and within one larger landslide, various types of slope movements interacting mutually in their development may be generated.

Devechi landslide, Azerbaijan

A motorway was inappropriately routed in a cut section at the bottom of 70 m high slope in the area between the toe of the slope and the village of Devechi. A rather large landslide was triggered. There was no time to develop a conceptual model, an observational model had to be developed directly on site. The first important finding was based on the analysis of the inclination of the slope. It was found on site that the slope was generally made up of two gradients; in the upper part the inclination was 30°, in the central and lower part it was 18–20° (Fig. 1). The landslide was formed in the central and lower part of the slope with a gradient of 18–20°. Further investigation discovered that the slope gradients reflected its geological structure (Novotný 2011).

The documentation of outcrops and of one trial pit in the central part of the slope together with the interpretation of landslide morphology helped to understand the landslide structure and mechanism. The upper part of the slope with a gradient of up to 30–35° consisted of loess loam; the slope gradient corresponded to the shear strength of loess loam. The central and lower part of the slope consisted of marine sands which contained horizontally bedded claystone interlayers. It is this presence of clayey layers (schematically presented in Fig. 1) which condition the slope gradient in this part as well as the stability behaviour. Further investigation showed that long-term slope processes pulled the clayey interlayers out of their original horizontal position, creating a layer of clay with high plasticity parallel to slope gradient. This layer was deposited between the original underlying strata of horizontally bedded marine sands and claystones and the overburden of silty colluvium derived from loess

loams. In the middle and lower parts of the slope the slope gradient adjusted in the long-term to an angle corresponding to the weakest point of the rock structure, which was the layer of high plasticity clay. The slip surface parallel to the slope gradient was found at a depth of 6–8 m and was connected to the layer of high plasticity clay. There was no groundwater in the landslide, and the drained long-term slope stability was conditioned by the clay layer, controlled by critical state friction angle.

The movement along the planar slip surface within the clay layer parallel to the slope gradient was also reflected in the landslide morphology, where signs of rotation, which would mean movement along a deeper curved slip surface, were missing.

The development of the landslide was also influenced by tectonic disturbances of the slope. The engineering geological documentation of the outcrops at the slope and at the landslide showed that the slope was disturbed by steep discontinuities. These discontinuities have directions corresponding to the directions of regional tectonic structures (transverse fractures of the Caucasus in the NW–SE and NE–SW direction, developed later as a result of the extrusion of the Turkish and Iranian block (Nyman et al. 2004)). This weakening of the slope was partially reflected in the trapezoid shape of the landslide as well as in the orientation of its internal cracks.

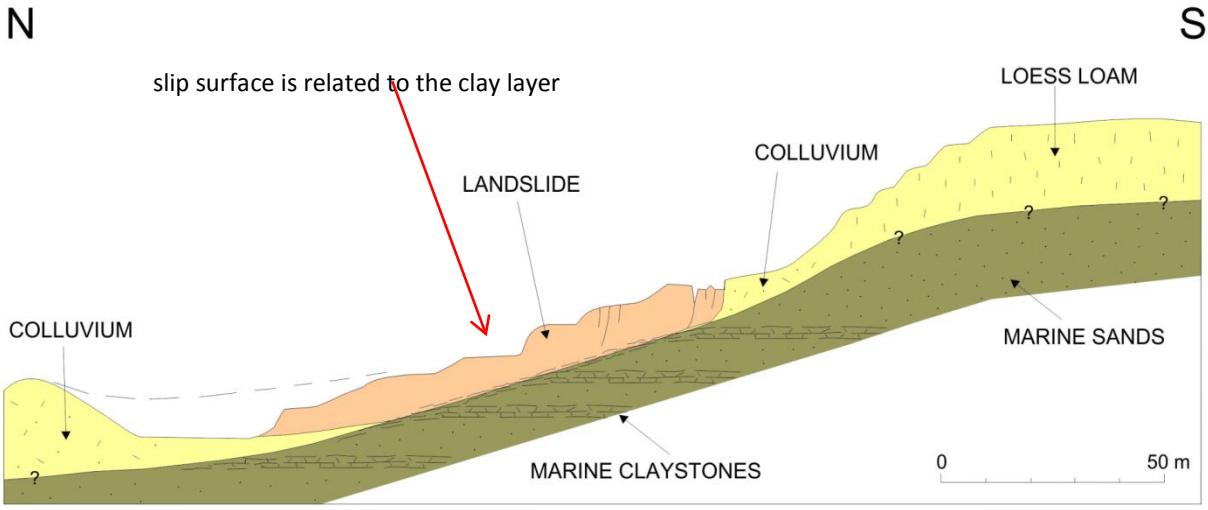

Fig. 1: Generalized section of the landslide near Devechi

Fig. 2: Overall view of the landslide

Fig: 3: Gas and water pipelines crossing a tension crack of the landslide, with the village of Devechi in the background

Březno landslide, Czech republic

An observational model of the Březno lanslisde is presented on Fig. 4. The model was constructed by the author using a cross section from a site investigation report (in Pašek 1974), an aerial view by Google and field mapping carried out by the author.

By sliding along the rotational surface of rupture ("rock slump" according to Varnes 1978, rotational landslide according to Nemčok et al. 1972), the Cretaceous marlstone block was pushed into the river bed, substantially narrowing it in this area. The main cause of the landslide, besides lithology prone to sliding, was primarily the erosive activity of the Ohře River which to this day maintains the whole landslide in a destabilized state. A layer of baked clays located in shallow depth below surface also plays an important role, preventing the area from being denuded into a gentle slope less prone to sliding.

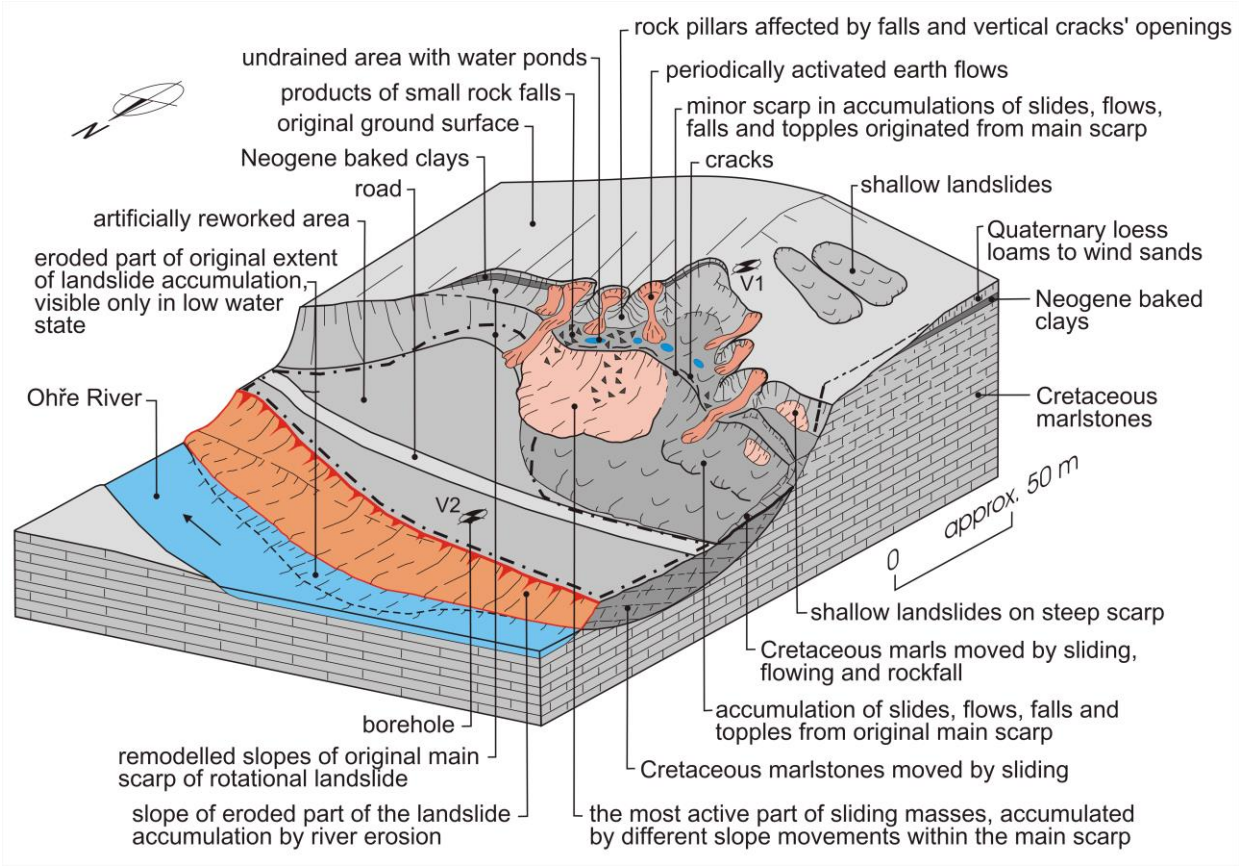

Fig. 4: Observational model of the Březno landslide in Cretaceous marlstones (Novotný 2014)

Unlike the simple structure of the rotational landslide, the morphology of the headscarp, resulting from various slope processes, is considerably complex. The headscarp above the rotated block is divided into a series of ridges separated by areas with periodical occurrence of minor landslides and notably of earth flows (Fig. 6). In long-term conditions, the ridges themselves are also unstable (Fig. 5), prone to rock fall and to opening of vertical tension cracks which can lead to rock toppling of large blocks (Fig. 7). The material from minor landslides, earth flows, rock falls and rock toppling accumulates at the toe of the slope of the headscarp and is not stable (Fig. 8). This instability is manifested by shallow landslides in this part. In the upper part of the accumulations, minor scarps are formed; above them, the terrain locally dips towards the slope, creating undrained basins that further destabilize the slope by the process of water infiltration into the unstable masses. Simultaneously, material from minor landslides, earth flows, rock falls and rock topples accumulated at the toe of headscarp slope adds weight here, thus destabilizing the entire landslide.

Fig. 5: Rock pillar affected by openings of cracks

Fig. 6: Earth flow

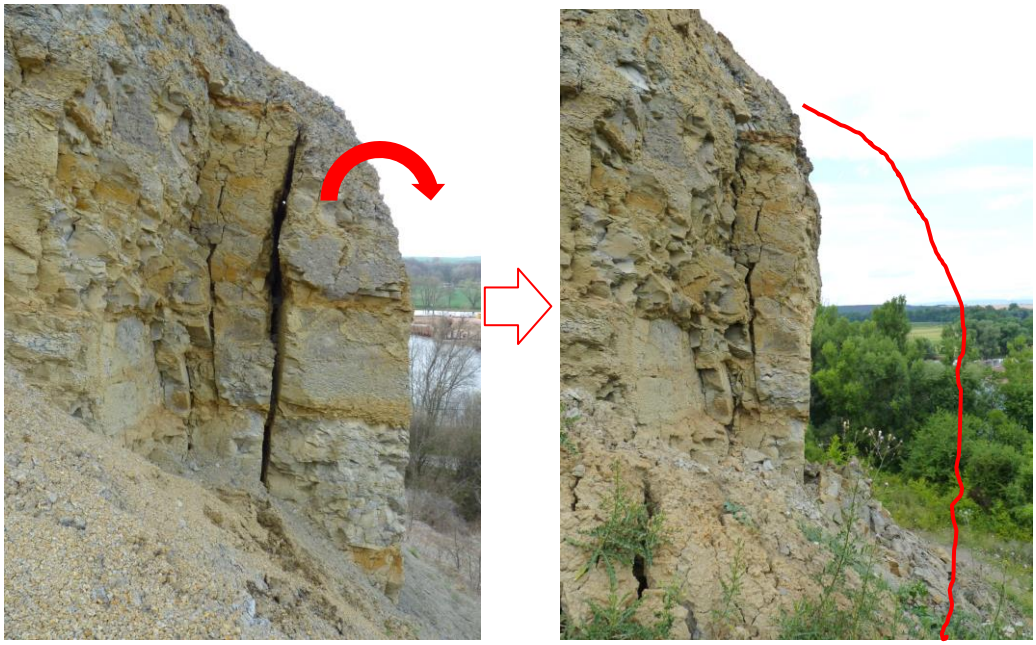

Fig. 7: Toppling of vertical blocks

Fig. 8: Scarp in sliding accumulations of slides, flows, falls and toppling

References

CRUDEN, D, LAN, H. X.: Using the Working landslide Classification of landslides to Asses a Danger from a Natural Slope. 12th IAEG Congress Torino 2014, G. Lollino et al. (eds.), Engineering Geology for Society and Territory – Volume 2, DOI: 10.1007/978-3-319-09057-3, Springer International Publishing Switzerland 2014, pp. 3–12, 2014

NEMČOK, A., PAŠEK, J., RYBÁŘ, J.: Classification of Landslides and Other Mass Movements. Rock Mechanics 4, pp. 71–78, 1972

NOVOTNÝ, J.: Stability Problems in Road and Pipeline Constructions and Their Mitigation ─ Examples from Sakhalin and Azerbaijan. Journal of Mountain Science (2011) 8: 307–313, DOI: 10.1007/s11629-011-2092-9, Science Press and Institute of Mountain Hazards and Environment, CAS and Springer-Verlag Berlin Heidelberg 2011

NOVOTNÝ, J.: Engineering Geological Models – Some Examples of Use for Landslide Assessments, 12th IAEG Congress Torino 2014, G. Lollino et al. (eds.), Engineering Geology for Society and Territory – Volume 7, DOI: 10.1007/978-3-319-09303-1_2, Springer International Publishing Switzerland 2014, pp. 11–15, 2014

NYMAN, D.J., THENHAUS, P.C., MOSCARDA, G. 2009. Mitigation of fault Crossing Hazards for the AGT Pipelines Project through Azerbaijan and Georgia. Terrain and geohazard challenges facing onshore oil gas pipelines, Thomas Telford, London, 468–479

PARRY, S., BAYNES, F.J., CULSHAW, M.G., EGGERS, M., KEATON, J.F., LENTFER, K., NOVOTNÝ, J., PAUL, D.: Engineering geological models: an introduction: IAEG commission 25. Bull Eng Geol Environ (2014) 73:689–706, DOI 10.1007/s10064-014-0576-x

PAŠEK, J.: Sesuvy středního Poohří (Landslides in the middle course of the Ohře river valley). Journal of Geological Sciences, Hydrogeology, engineering geology, 11, pp. 53–79 (in Czech), 1974

VARNES, J. D.: Slope Movement Types and Processes. In: Landslides, Analysis and Control, Special Report 176, editors: R. L. Schuster, R. J. Krizek, National Academy of Sciences, Washington, D.C., pp. 11–33, 1978

Slow deep landslides in Southern Italy: failure mechanisms and predisposing and triggering factors

F. Cotecchia *, F. Santaloia **, C. Vitone *, O. Bottiglieri *, G. Pedone *
Technical University of Bari, Italy*
IRPI-CNR – Bari, Italy **

1. Introduction

The assessment of landslide hazard provides knowledge about both the location of a given hazard degree and the appropriate mitigation strategy, if based on a deterministic recognition of the processes that may determine the susceptibility of slopes to be location of landsliding (Corominas and Moya 2008; Fell et al. 2008a-b; Cascini 2008; Cotecchia et al. 2014a-c). Such deterministic assessment can be pursued through the interpretation and hydro-mechanical modelling of the slope equilibrium, implementing all the geo-hydro-mechanical factors characterizing the slope.
In practice, though, the assessment of landslide hazard is still seldom dealt with geo-hydro-mechanical modelling.
The urgency of the dissemination of training in the diagnostic of landslide hazard making use of such a geotechnical approach is made evident by the still numerous deaths due to landslide phenomena, despite the diffusion of regional landslide risk mapping (Fell et al. 2005; Leroi et al. 2005; Lollino et al. 2014). This is mostly due to the complexity of the slope as geotechnical system, so that seldom the model can represent the whole complexity of the slope; rather, experienced selection of the most relevant factors and processes to be addressed in the modelling is required.
Both past and recent experience in the diagnosis of landsliding has revealed that the features of slope failure vary with the varying features of the slope geo-hydro-mechanical factors, resulting in different classes of landslide. Hence, a rational approach to slope modelling requires a strong synergy between experts in geomorphological and phenomenological slope studies and experts in numerical analyses of the slope processes. Such synergy allows for model simplifications with respect to reality, but keeping numerical modelling strictly connected to the site evidences.
Following these premises, a stage-wise methodology for the assessment of landslide hazard at the slope scale will be presented, which is quantitative and based on the knowledge of slope hydro-mechanics. The methodology will be exemplified by presenting its application for some case histories located in Southern Italy, which are representative for different classes of slope failure mechanism.

2. The Tolve landslide (Southern Apennines)

The Tolve landslide is a case of delayed failure (Figure 1) due to foot excavation of a slope in stiff highly overconsolidated and strain softening clays (Cotecchia et al. 2004; 2014b), i.e. the Sub-Apennine Blue Clays. Landsliding occurred in a very gentle slope (Figure 1, 8° average inclination), 12 years after a 3 m deepening of a road at the toe, mobilizing the landslide bodies recalled as 1, 2 and 3 in the geo-morphological map in Figure 1. Two of the landslide bodies are very large and, since the start, were considered to be comparably deep and not to

result from a first failure triggered solely by the comparatively small road excavation. Therefore, since the first stage of the study, the landslide mechanism was expected not to be a first delayed failure in stiff clays due to foot excavation.
Figure 2 shows the geological section a-a of the slope, as derived from the analysis of continuous coring down several boreholes. Piezometric monitoring and modelling of the uncoupled seepage in the slope was carried out by means of a FEM code. Limit equilibrium analyses were conducted too, assuming pore pressure distributions coming from the seepage modeling, which give evidence to a strong impact of the seepage on the slope stability, then recognized to be a factor predisposing the slope to landsliding. Nonetheless, the slope is verified to be stable in the limit equilibrium analyses when assuming first failure, i.e. implementing strength parameters between peak (e.g. c'_p = 81kPa, ϕ'_p = 15° for the deep Blue Clays) and post-peak (c' = 0kPa, ϕ' = 15°). Limit equilibrium analyses hence prove that the Tolve slope was not experiencing first failure after foot excavation, rather, it was probably experiencing a reactivation.
Geomorphological analyses provided evidence (Guerricchio et al. 2000) of the inclusion of the landsliding within a larger paleo-landslide basin, with toe at bottom of the river valley and perimeter as shown in Figure 1, which had been probably generated in the Quaternary by river erosion and tectonic tilting. It could be then recognized that the new landsliding was mobilizing the North-eastern portion of paleo-landslides, with a new toe at the road.
The current activity style of the landslides was investigated by means of geomorphological surveys and inclinometric monitoring (Figure 1). The phenomenological interpretation of the landslide mechanism allowed for arguing that the new landsliding had resulted from a progressive failure starting from the bottom of the road excavation and reaching, with time, the two paleo-shear bands pre-existing at depth in the slope (bodies 2 and 3 in Figure 1). While body 1 had moved first, bodies 2 and 3 could move only when the new portion of the slip surface had fully developed.
Limit equilibrium back analyses and numerical modelling of section a-a, the latter using FEM code Plaxis 8, have validated the phenomenological interpretation (Cotecchia et al. 2014b).

3. The Petacciato landslide basin (southern Adriatic coast)

A large landslide basin, about 4 km^2 wide, occurs on a slope located along the Adriatic coastline, just below the town of Petacciato. Figure 3 shows the geo-morphological map of the hill-slope, as resulting from geological and geomorphological surveys, analysis of corings and aerial photo interpretation, all of them resulted to be crucial for the phenomenological interpretation of landsliding. The boreholes (Figure 3) were equipped with either piezometers, down to 119 m depth, or inclinometers, some of which deeper than 100 m, and monitoring was on from 1982 to 2004 (Cotecchia et al. 2008, 2014b). Laboratory testing was carried on undisturbed samples.
Stiff Sub-Apennine Blue Clays form most of the hill-slope, outcropping in the lower part of the slope and underlying debris in the resting part. The Blue Clays, less or more sandy, were found to be characterized by peak strength parameters equal to c'_p=40-160kPa and ϕ'_p=18°-22° and residual friction angle about 10° (Cotecchia et al. 2014b).
The morphology of the slip surfaces of the several shallow to deep landslide bodies active in the slope (Figure 4) has been first derived from the analysis of the borehole corings and of the inclinometric monitoring data, as requested by the proposed methodology. Given the slope gradient and the strength of the clays when undisturbed, the mobilization of such bodies is

possible only if the operational strength along the reconstructed slip surfaces is between post-peak and residual, according to limit equilibrium back analyses, as for a reactivation of landsliding rather than a first failure. Such hypothesis was validated by studies of the paleogeographic evolution of the slope, according to which the stretch of coast here of reference was involved in landsliding in the Quaternary, in connection with the sea level excursions during the glaciations. The toe of these paleo-landslides is generally off-shore the present coastline.
Piezometric monitoring has given evidence to very large piezometric levels at large depths in the slope, higher that those measured at shallow depths. As such, piezometric heads can be recognized to be a factor impoverishing the strengths available at large depth in the slope and predisposing the slope to deep sliding. Further factor bringing about a reduction of the intrinsic strength properties of the clays with depth is the larger plasticity index of the deep clays, with respect to that of the shallow ones.
As resulting from the temporal analyses (with historical documents, maps and multi-year aerial photos), a wood had been covering the slope up to the beginning of the XX century (De Filippo 2000) and only after the cut of this wood intermittent landsliding started. Fifteen main events have been recorded from 1906 to 2009, in late winter - early spring. The largest movements have generally occurred at the slope toe, damaging both the railway and the motorway, being followed by a retrogression of movements, to reach the Petacciato village at the top within few days maximum (Cotecchia et al. 2014b).
The phenomenological interpretation has hence suggested that the smaller bodies at the toe of the slope and the larger one have been remobilized since early 20th century due to a variation in piezometric conditions generated by the cut of the wood on the hill-slope and that, since this external action, a new toe has developed from a new failure, which has joined the coastline with pre-existing slip surfaces in the slope, as found also in the Tolve case study. After the formation of the new toe, the reactivation events have been seasonal, probably triggered by the seasonal feeding of the seepage domain by the cumulated infiltration of rainfalls from autumn to early spring (Cotecchia et al. 2009, 2014b), which generate increase of the piezometric heads and strength decay.
Limit equilibrium back-analyses of the active sliding bodies have confirmed the phenomenological interpretation.
.

4. Landsliding in clayey flysch

The soils outcropping within chain areas, namely areas that have been location of orogenesis, have generally experienced severe tectonic processes. This is the case of the soils within the Apennines in southern Italy, a chain area part of one of the most important and still active thrust systems in the Mediterranean. The Pisciolo landslide and the Santa Croce di Magliano landslide are two case histories representative of landsliding in this geo-mechanical context, where slopes are formed of tectonized clayey soils, predisposing the slopes to instability.

4.1. A framework of behaviour for fissured clays

The characterization of fissured clays has ever since been a major task for geotechnical research (Terzaghi 1936; Lo 1970; AGI 1979; Cicolella and Picarelli 1990; Marsland 1971; Petley 1984; Fearon and Coop 2000, 2002; Picarelli and Olivares 2004; Hight et al. 2007; Silvestri et al. 2007; Farulla et al. 2010). Recent research has been carried out with the aim of assessing a basic simple framework of the influence of fissuring on the mechanics of clays

(e.g. Cotecchia and Santaloia 2003; Vitone 2005; Cotecchia et al. 2007; Cotecchia and Vitone 2011; Vitone and Cotecchia 2011), to be addressed in practice for the prediction of the strength reduction stemming from fissuring. The fissuring features have been codified by means of a characterization chart, which accounts for both the lithology and consistency of the soil matrix and the discontinuity features.
The applicability of continuum mechanics to characterize clays of medium to very high fissuring intensity, hence the extent to which element test results can be of use to model their behaviour, has been verified by means of full field measurements, through either the False Relief Stereophotogrammetry method (Desrues and Viggiani 2004; Vitone et al. 2009), or Digital Image Correlation techniques (Vitone et al. 2012, 2013 a, b). These measurements have shown that, within Representative Element Volumes (REV), the development of shear bands across the specimen takes place similarly to what observed for unfissured clays. Therefore, for the fissure identities of reference, the element test data can be used according to traditional soil mechanics, as for unfissured clays.
The compression curve of the fissured clay is found to lie on the left of the Intrinsic Compression Line (ICL, Burland 1990) of the reconstituted clay up to high pressures; hence, the fissured clay does not enter the so-called structure permitted space (Leroueil and Vaughan 1990), possible only for sensitive unfissured clays. Cotecchia and Chandler (2000) introduced, for unfissured clays, the stress sensitivity ratio, $S_\sigma = p'_y / p^*_e$ (ratio between the mean effective stress at gross yield in isotropic compression, p'_y, and the equivalent pressure on the isotropic normal consolidation curve of the reconstituted clay, p^*_e) to quantify the influence of microstructure on the clay gross yielding, where gross is a term used to distinguish the yielding preceding major plastic straining and occurring about the state boundary surface (Cotecchia and Chandler 2000) from the first yielding. This parameter has resulted to be $S_\sigma \geq 1$ for unfissured sensitive clays, this implying that the natural microstructure may provide the clay with a larger state boundary surface and larger strength with respect to the reconstituted. Instead, for clays of whatever microstructure, but whose mesofabric includes fissuring, the effect of the structure (from micro to meso) brings about $S_\sigma < 1$ (Vitone and Cotecchia 2011). Hence, for fissured clays, even when the microstructure is strong with respect to that of the reconstituted, its influence on the clay mechanics is overcome by fissuring. The latter makes the clay not only weaker than the corresponding unfissured clay, but also weaker than the clay when reconstituted.
.

4.2 The Pisciolo clay slides (Southern Apennines)

Phenomenological analyses of the Pisciolo hill-slope (Cotecchia et al. 2014a-c; Figure 5) have shown that it is formed of sedimentary successions deposited in a pre-orogenic marine basin (Cretaceous-Miocene). Direct and indirect investigations, consisting in borehole coring and bi-dimensional resistivity surveys respectively, have shown the hill-slope to be formed of fissured clays interbedding discontinuous calcarenite and sandstone intervals (Paola Doce Formation). Sandstones of the Numidian Flysch cover locally these materials (Figure 5).
The stereoscopic analysis of multi-temporal aerial photos gave evidence to a strong evolution of landsliding on the hill-slope from 1955 to present, with enlargement and deepening of the landslide bodies. In particular, more than 8 active landslide bodies have been identified on the slope (Figure 5), whose shear bands have been detected by some of the inclinometers installed. The landslide bodies have been found to be from medium to large depth, the most active ones (C and C9) being located in the southern part of the landslide basin, where an underground pipeline (4m depth) experienced severe damage in the last 10 years. These

landslides are characterized by sliding velocities that range from 1.2 to 18 cm/year and depths larger than 30 m. Bodies C and C9 are nested at the toe of a deeper (50-60 m depth) and slower (mean velocity of 1 cm/year) landslide body, of retrogressive evolution. Other three very active landslide bodies occur in the northern portion of the hill-slope (F, L and G), of medium depth and displacement rate of few mm/month.
The phenomenological analyses have envisaged that, apart from body F, that was already present in 1955, all the other landslide bodies are result of first failure progression in the hill-slope. In particular, bodies C9, C and A result from the enlargement of soil slips with toe about a gorge, the latter originally present in the hill-slope and guaranteeing a higher efficiency of the superficial drainage. This has been progressively filled by solid transport and reduced in section due to landslide movements, as to not guarantee the original drainage any more. This loss may have predisposed the slope to an increase in infiltration of rainfalls, with a consequent increase in the piezometric heads, that are currently high, down to large depths, in the most active portions of the hill-slope.
All the landslide bodies mainly involve fissured clays, whose hydro-mechanical properties have been characterized in the laboratory (Cotecchia et al. 2014a-c). Fissuring strongly influences the hydro-mechanical response (Vitone and Cotecchia, 2011; Vitone et al. 2012, 2013a-2013b) of these highly plastic (PI=33-45%) and active (A=0.8-0.9) clays (clay fraction=40-52%, silt fraction=35-36% and sand fraction=11-21%), because it increases their permeability ($k \geq 10^{-9}$ m/s) and reduces their shear strength (mean strength parameters: $\varphi'_p=20°$ for $c'_p=0$ kPa).
Limit equilibrium analyses, conducted with reference to the in situ piezometric measurements, confirmed that bodies C and A are at first failure, since their activity currently mobilizes $\varphi'_m \cong \varphi'_p$. This is not the case for body F, for which $\varphi'_m \leq \varphi'_{post\text{-}peak}$.
Both the inclinometric and GPS monitoring have shown that the displacement rates of landslide bodies C9 and C vary seasonally, with maximum values at the end of winter/early spring. These maximum velocities have been recorded in conjunction with the maximum pore pressure values, that are found to follow seasonal fluctuations in 15 piezometric cells installed down to 80 m depth in the hill-slope (Cotecchia et al. 2014c). This finding has suggested that the piezometric heads in the hill-slope are influenced significantly by the seasonal infiltration of water, allowed for by the permeability of the slope system, that is affected not only by the fissuring of the clays, but also by the coarser soil strata and the fractured rock blocks floating within the clays, that make the slope more prone to rainfall infiltration.
FEM analyses have validated the phenomenological interpretation of the effects of the soil-atmosphere interaction recorded in the field.
.

4.3. The Santa Croce di Magliano landslides

At SCM the slopes are formed by turbidites part of the Daunia Unit and are diffusely location of failure processes. These start in the scaly clay strata (SCM scaly clay soils), whose mesofabric and geotechnical properties have been discussed above. Thereafter they involve the BENT clays and the FAE rock slab upslope. Most of the sliding surfaces have toe about the river flowing at the bottom of the valleys, either North or South the village. Several springs occur about the rock-clay contact, which represent the outcropping of a seepage domain present in the slopes, whose water table occurs at 2-3 m depth downhill.
The SCM scaly clays, along with the BENT clays, are of even higher plasticity than the SEN and PI clays. For these intrinsically weak clays, fissuring provides a further source of strength reduction. Furthermore, at SCM the slope strengths do not benefit from the presence of as

many coarse strata and floating rock beddings, as for both the SEN and the PI slopes. Within these simpler sequences, the recognized landslide mechanisms are mainly roto-translational sliding, as shown by the inclinometer data. This inclinometer intercepted a sliding surface at 22 m depth in a southern slope, along which the displacement rates recorded were about 14 mm/month during a period of high landslide activity. The failure mechanism recognized in the slope may be considered representative of the landsliding for most of slopes at SCM (Cotecchia et al. 2007; Cotecchia et al. 2014c).

The landslide activity seems to differ between the northern and the southern slopes of the SCM promontory. Long-term landsliding has involved the northern slopes, reaching and involving the top FAE rock slab, so as to cause the movements of several rock blocks. Conversely, the landsliding in the southern slopes appears more recent and causing more limited variation of the original morphologies. The back-analyses of the northern landslides result in mobilised friction angles ϕ'_m=17°–18° (c' = 0 kPa), which are far above the residual friction angle of the clays and only a bit lower than the clay peak friction angles on the dry side (Cotecchia et al. 2003, 2007, 2014c). Conversely, the mobilized friction angles for the southern landslides are smaller, ϕ'_m=12°-13°.

The high operational strengths in the northern slopes may appear to be in contrast with the more mature activity of landsliding in such slopes. However, it should be considered that the intense landsliding has been active for so long in these slopes, as to cause at least partial remoulding of the scaly clays. Remoulding may have caused an increase in the shear strength of the clays, as expected according to the framework of behaviour of fissured clays. This remoulding has not taken place yet in the southern slopes of the promontory, which are then likely to be weaker than at North.

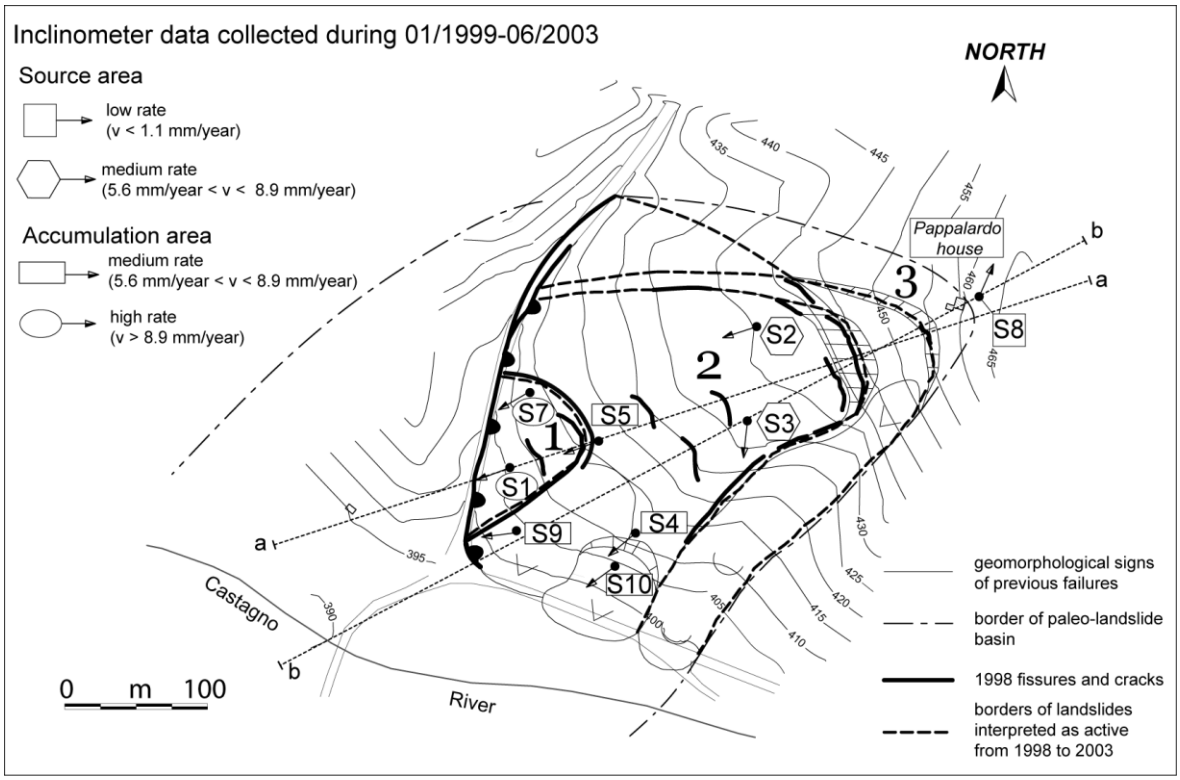

Figure 1. *Geomorphological map of the Tolve slope (after Guerricchio et al. 2000 and Cotecchia et al. 2014b).*

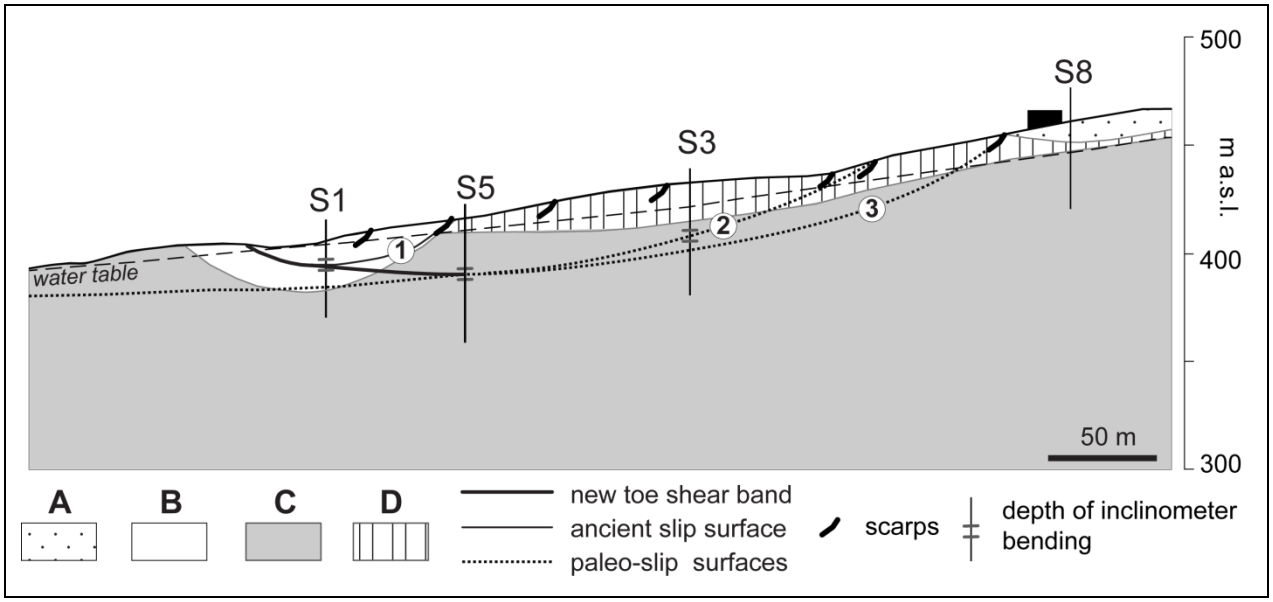

Figure 2. *Geological and geomorphological section a-a of the Tolve slope (section axis in Figure 9). Key: soil complexes: A) yellow sands, B) remoulded clays, C) Blue Clay, D) weathered clays (after Cotecchia et al. 2014b).*

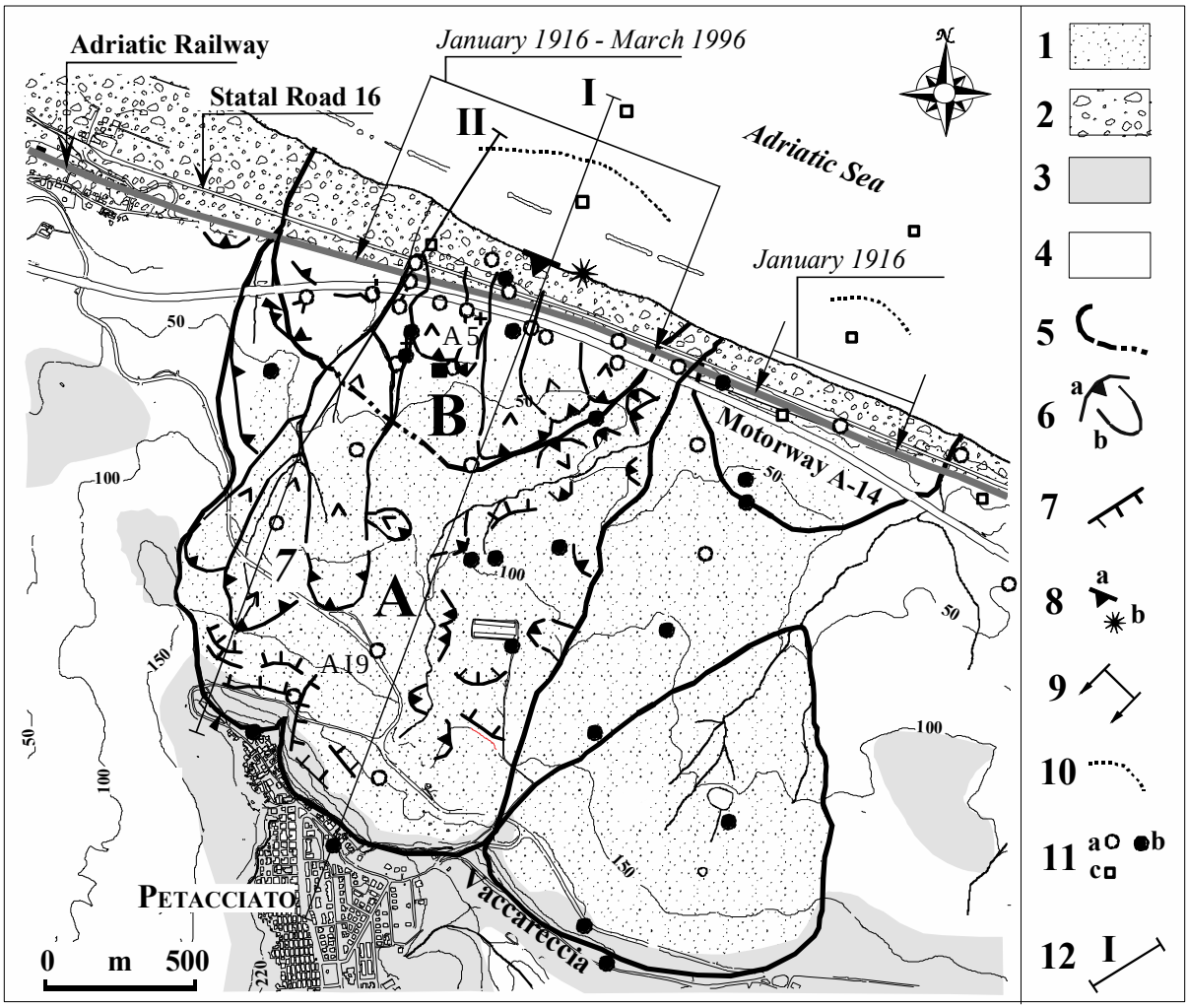

Figure 3. *Geomorphological map of the Petacciato slope (after Cotecchia et al., 2009, 2014b). Key: 1) colluvium or landslide deposits, 2) beach deposits, 3) Alluvial and marine*

deposits, 4) Sub-Apennine Blue Clays, 5) boundaries of the deep landslide bodies (a: crown, b: boundary of the body), 6) shallow to intermediate depth slides, 7) ground failures, 8) clay mound (a) and uplifted reef (b), 9) stretch of the railway tracks most damaged during last century landsliding, 10) ancient landslide toes, 11) field investigations (a: inclinometer, b: piezometer, c: un-equipped borehole), 12) line of section.

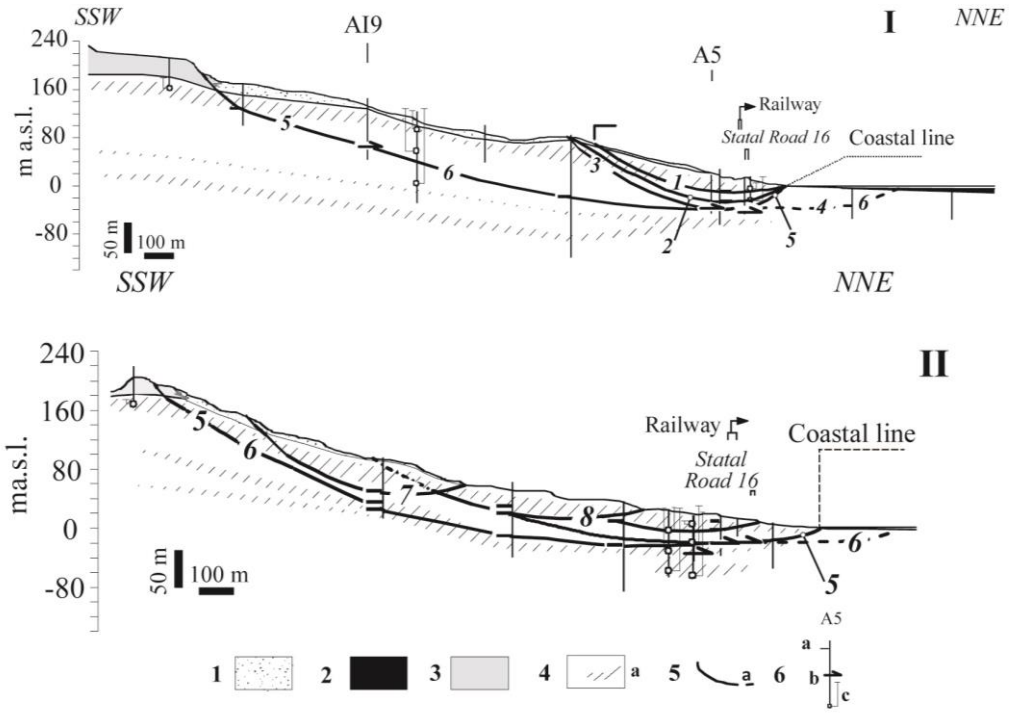

Figure 4. *Cross sections of the western portion of the Petacciato basin (Cotecchia et al. 2014b). Key: (a); section axes in Figure 14. Key: 1) colluvium or landslide deposits, 2) present marine deposits, 3) Alluvial and marine deposits, 4) Sub-Apennine Clays (a: sandy-silty intervals), 5) sliding surfaces (a: ancient slip surface), 6) boreholes (a: sheared and fractured zones, b: inclinometer shearing, c: piezometric level).*

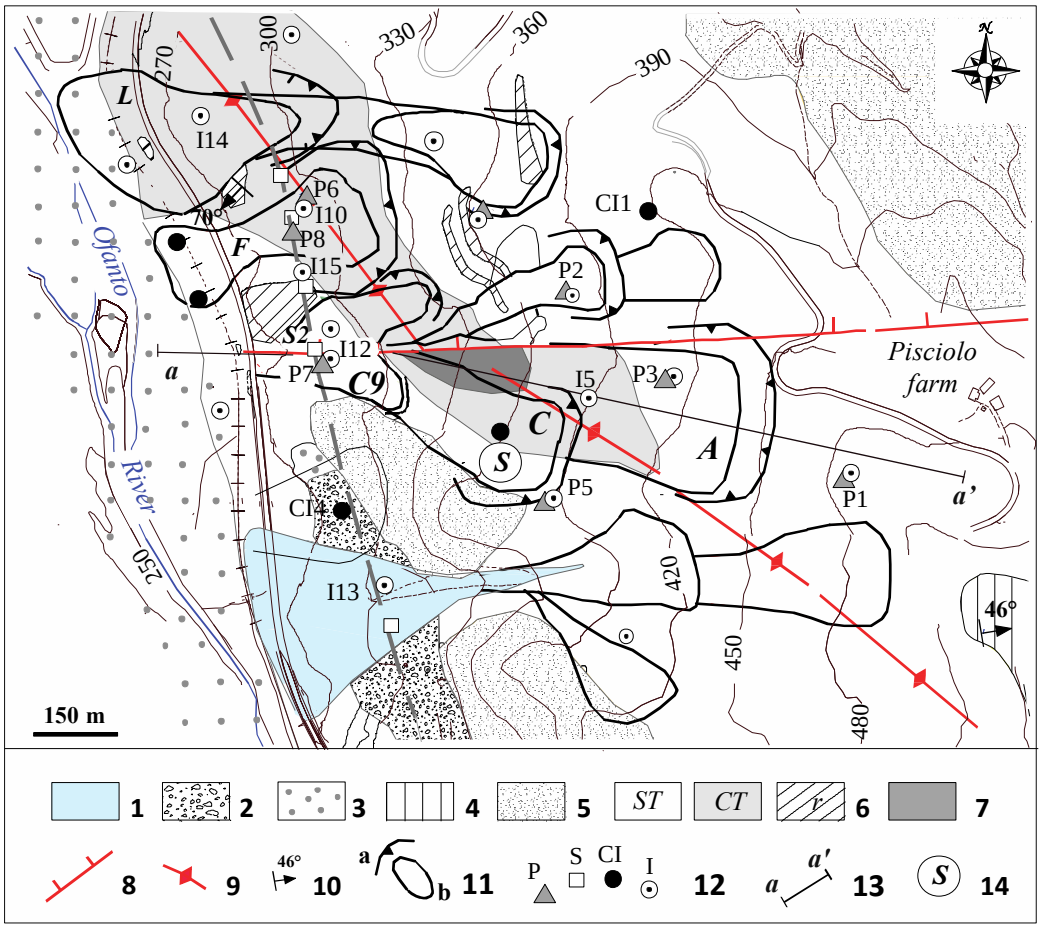

Figure 5. *Schematic geological map of the Pisciolo hill-slope. Key: (1) fan deposit; (2) debris deposit; (3) alluvial deposit; (4) Pliocene succession; (5) Numidian Flysch; (6) Paola Doce Formation: ST-sandy sub-complex, CT- calcareous sub-complex, r-rocky strata; (7) Red Flysch; (8) fault; (9) anticline axis; (10) attitude strata; (11) landslide: a-crown, b- body; (12) P: continuously cored borehole equipped with piezometers, S: GPS sensor; CI: continuously cored boreholes equipped with inclinometer casing, I: destructive boreholes equipped with inclinometer casing; (13) line of the modelled section in Figure 17; (14) sampling of outcropping clays for the water retention curve determination (Cotecchia et al., 2014c).*

References

AGI (1979) Some Italian experiences on the mechanical characterisation of structurally complex clay soils. In International Society of Rock Mechanics (ed.), Int Soc Rock Mech 4th Int Cong 1, pp 827-846

Burland JB (1990) On the compressibility and the shear strength of natural clays. Géotechnique 40(3):329-378

Cascini L (2008) Applicability of landslide susceptibility and hazard zoning at different scales". Engineering Geology, 102, 164–177

Cicolella A, Picarelli L (1990) Decadimento meccanico di una tipica argilla a scaglie di elevata plasticità. Italian Geotechnical Journal 24:5-23

Corominas J, Moya J (2008) A review of assessing landslide frequency for hazard zoning purposes, Engineering Geology, 102, 193–213

Cotecchia F, Chandler RJ (2000) A general framework for the mechanical behaviour of clays. Géotechnique 50(4):431-447

Cotecchia F, Cafaro F, Melidoro G, Mitaritonna G (2003) Mechanical behaviour of natural tectonized bentonites. Proc Int Workshop Geotechnics of Soft Soils, Amsterdam, pp 397-402

Cotecchia F, Lenti V, Bottiglieri O, Cafaro F (2004) Analysis of a delayed re-activation of movements on a stiff clay slope in Southern Italy after foot excavation. Proc 11th Int Symp on Landslides, Rio de Janeiro, Brazil, 1207-1214

Cotecchia F, Vitone C, Cafaro F, Santaloia F (2007) The mechanical behaviour of intensely fissured high plasticity clays from Daunia. Proc 2nd Int Workshop Characterisation and Engineering Properties on Natural Soils, Singapore, Taylor & Francis London, pp 1975-2003

Cotecchia F, Santaloia F, Bottiglieri O, Monterisi L (2008) Landslides in stiff clay slopes along the Adriatic coast (Central Italy). Proceedings of the 11th International Symposium on Landslide, Xian, China, 2, 1525-1531

Cotecchia F, Mitaritonna G, Elia G, Santaloia F, Lollino P (2009) Meccanismi di frane in pendi in argille dell'Italia Meridionale ed effetti delle precipitazioni meteoriche. 1st Int Workshop on Landslides: rainfall induced landslide and nowcasting models for early warning system, pp 31-43

Cotecchia F, Santaloia F, Lollino P, Vitone C, Mitaritonna G (2010) Deterministic landslide hazard assessment at regional scale. Geoflorida. Advances in Analysis, Modeling and Design. West Palm Beach, Florida, 3130-3139

Cotecchia F, Pedone G, Bottiglieri O, Santaloia F, Vitone C (2014a) Slope – atmosphere interaction in a tectonized clayey slope: a case study. Italian Geotechnical Journal 1: 34-61

Cotecchia F, Santaloia F, Lollino P, Vitone C, Pedone G, Bottiglieri O (2014b) From a phenomenological to a geomechanical approach to landslide hazard analysis. European Journal of Environmental and Civil Engineering (EJECE - ISI). DOI 10.1080/19648189.2014.968744, In print

Cotecchia F, Vitone C, Santaloia F, Pedone G, Bottiglieri O (2014c) Slope Instability processes in intensely fissured clays: case histories in the southern Apennines – Landslides Journal, DOI 10.1007/s10346-014-0516-7, in print

De Filippo G (2000) Petacciato: il passato ritrovato [Petacciato: the rediscovered past]. Luciano editore

Desrues J, Viggiani G (2004) Strain localization in sand: an overview of the experimental results obtained in Grenoble using stereophotogrammetry. Int J Numer Anal Meth Geomech28: 279-321

Farulla CA, Ferrari A, Romero E (2010) Volume change behaviour of a compacted scaly clay during cyclic suction changes. Canadian Geotechnical Journal 47(6):688-703

Fearon R, Coop M R (2000) Reconstitution - what makes an appropriate reference material? Géotechnique 50(4): 471-477

Fearon R, Coop MR (2002) The influence of landsliding on the behaviour of a structurally complex clay, Quarterly Journal of Engineering Geology and Hydrogeology 35: 25-32

Fell R, Corominas J, Bonnard C, Cascini L, Leroi E, Savage WZ (2008a) Guidelines for landslide susceptibility, hazard and risk zoning for land use planning. Engineering Geology, 102, 85-98

Fell R, Corominas J, Bonnard C, Cascini L, Leroi E, Savage WZ (2008b) Guidelines for landslide susceptibility, hazard and risk zoning for land-use planning. Commentary. Engineering Geology, 102, 99-111

Fell R, Ho KKS, Lacasse S, Leroi E (2005) A framework for landslide risk assessment and management. In O Hungr, R Fell, Couture R, Eberhardt E (Eds), Landslide Risk Management. London: Taylor & Francis, 3–26

Guerricchio A, Melidoro G, Panaro V (2000) Deformazioni gravitative dei versanti nel territorio comunale di Tolve (Basilicata). Bulletin Italian Geological Society, 10-20

Hight DW, Gasparre A, Nishimura S, Minh NA, Jardine RJ, Coop MR (2007) Characteristics of the London Clay from the Terminal 5 site at Heathrow Airport. Géotechnique 57(1): 3-18

Leroi E, Bonnard C, Fell R, McInnes R (2005) Risk assessment and management. In O Hungr, R Fell, Couture R, Eberhardt E (Eds), Landslide Risk Management. London: Taylor & Francis, 159–198

Leroueil S, Vaughan P (1990) The general and congruent effect of structure in natural soils and weak rocks. Géotechnique 40(3):467-488

Lo KY (1970) The operational strength of fissured clays. Géotechnique 20(1):57-74

Lollino P, Cotecchia F, Elia G, Mitaritonna G, Santaloia F (2014) Interpretation of landslide mechanisms based on numerical modelling: two case-histories; European Journal of Environmental and Civil Engineering (EJECE – ISI), DOI: 10.1080/19648189.2014.985851, In print

Marsland A (1971) The shear strength of stiff fissured clays. Roscoe Memorial Symp, Cambridge Univ, pp 59-68

Petley DJ (1984) Shear Strength of Over-Consolidated Fissured Clay. Landslides; Proc Int Symp, 2, pp 167-172

Picarelli L, Olivares L (2004) Mechanical behaviour of highly sheared clay shales. Advances in Geotechnical Engineering: The Skempton Conference - Advances in Geotechnical Engineering, ICEl, pp 580-591

Terzaghi K (1936) Stability of slopes in natural clays. Proc. 1st Conf. On Soil Mechanics, Harvard, 1: 161-185

Silvestri F, Vitone C, d'Onofrio A, Cotecchia F, Puglia R, Santucci de Magistris F (2007) The influence of meso-structure on the mechanical behaviour of a marly clay from low to high strains. Geotechnical Tatsuoka Symposium, Rome, Hoe I Ling et al eds, Soil Stress-Strain Behaviour: Measurement, Modelling, Analysis, Springer, the Netherlands, pp 333-350

Vitone C, Cotecchia F (2011) The influence of intense fissuring on the mechanical behaviour of clays. Geotéchnique 61(12):1003-1018

Vitone C, Cotecchia F, Desrues J, Viggiani G (2009) An approach to the interpretation of the mechanical behaviour of intensely fissured clays, Soils & Foundation Journal 49(3):355-368

Vitone C, Cotecchia F, Viggiani G (2012) Localisation processes and size effects for fissured clay specimens. Advanced Multiphysical Testing of Soils and Shales (AMTSS) Workshop In Springer Series in Geomechanics and Geoengineering, Laloui Ferrari Eds, pp 219-225

Vitone C, Cotecchia F, Viggiani G, Hall SA (2013a) Strain fields and mechanical response of a highly fissured bentonite clay, Int J Numer Anal Meth Geomech 37:1510-1534

Vitone C, Viggiani G, Cotecchia F, Hall SA (2013b) Localized deformation in intensely fissured clays studied by 2D digital image correlation, Acta Geotechnica 8:247-263

Analysis of a volcanic ash slope subjected to wetting and drying cycles

Lyesse LALOUI, Alessio FERRARI, Chao LI, John EICHENBERGER

Swiss Federal Institute of Technology, Lausanne, EPFL, Switzerland

Abstract. Rainfall-induced landslides in volcanic ashes represent a major natural hazard in many densely populated regions around the world. Volcanic ashes in steep slopes are most of the time in a partially saturated state. Capillary effects greatly influence the soil behaviour. During rain infiltration, volcanic ashes display strong volume changes and shear deformations associated with the development of the failure mechanism. Environmental fluctuations and the consequent wetting and drying cycles in the slope are rarely considered. This paper presents a hydro-mechanical analysis of the behaviour of a volcanic ash slope subjected to daily wetting and drying cycles. A transient finite element simulation is performed with a 2D slope model that is representative for a landslide-prone volcanic area in Costa Rica. The ash behaviour is reproduced by means of the bounding surface and multi-mechanism elasto-plastic model ACMEG-s for unsaturated soils; the model was previously calibrated on the basis of a laboratory testing programme designed to characterise the hydromechanical behaviour of the volcanic ash. The results of the finite element simulation demonstrate the important role of wetting and drying cycles, slope geometry and bedrock on the evolution of matric suctions, soil volume changes and shear deformations.

Keywords. Hydromechanical modelling, Unsaturated soil, Volcanic ash, Wetting pore-collapse.

Introduction

Rainfall-induced landslides in steep slopes of volcanic origin are common around the world and have caused massive destruction and the loss of lives (Italy: [1, 2]; Hong Kong: [3]; Central America: [4-6]). In Central America, the populated areas surrounded by steep volcano slopes are highly vulnerable to rainfall- and earthquake-induced landslides that are triggered in loose volcanic soils. In 2001, the Las Colinas landslide in El Salvador claimed > 500 casualties [5], and in 1998, thousands of landslides were caused by Hurricane Mitch throughout all of Central America with > 9000 casualties [7]. Due to the loose structure from the depositional process, narrow grain-size distribution, degree of weathering and collapsibility, failed soil masses from volcanic deposits are often reported to turn into rapid flow slides or debris flows with catastrophic consequences in the runout zones [8]. At the origin, the involved materials are mostly in a state of partial saturation.

At the end of the wet season of 2005, two rainfall-induced landslides in volcanic ashes caused material damage and production losses in a quarry situated along the hillslopes of Irazu volcano in Costa Rica. In this paper, a physically-based, hydro-mechanically coupled continuum modelling approach is applied performing a 2D finite element slope model, aimed at reproducing the behavior of the landslide-prone site on the foothills of Irazu volcano in Costa Rica. Realistic rainfall conditions are considered, which reproduce in particular the intense, short-duration rainfall events during a typical wet season. Particular attention is paid

to the analysis of the spatial-temporal evolution of matric suctions, degree of saturation and unsaturated flow, as well as reversible and irreversible volumetric and deviatoric deformations induced by rainfall infiltration. Emphasis is placed on a realistic representation of the hydro-mechanical behaviour of volcanic ashes by means of an elasto-plastic constitutive model for partially saturated soils. An extensive laboratory testing programme was carried out [9] to characterise the hydro-mechanical behaviour of the involved volcanic ash and to calibrate the various model components, which are used in the modelling approach and the numerical analysis presented in this paper.

The hydro-mechanically coupled modeling framework

The ACMEG-s elasto-plastic constitutive model [10, 11] is used to reproduce the hydro-mechanical behavior of the volcanic ash. Along with the model for the soil water retention behaviour [12, 13], the constitutive models define the stress-strain and suction-degree of saturation relationship, respectively. Both these mechanical and hydraulic constitutive components are embedded in a generalized effective stress framework that is suitable to describe hydro-mechanically coupled processes in unsaturated and saturated conditions [14, 15]:

$$\boldsymbol{\sigma}' = \boldsymbol{\sigma} - p_a \boldsymbol{I} + S_r \left(p_a - p_w\right) \boldsymbol{I} = \boldsymbol{\sigma} - S_r p_w \boldsymbol{I} \qquad (1)$$

Where $\boldsymbol{\sigma}'$ is the effective stress tensor, $\boldsymbol{\sigma}$ is the total stress tensor, p_a (equal to zero) and p_w are the pore air and pore water pressure, respectively, and S_r is the degree of saturation.
In the ACMEG-s model the elastic volumetric and deviatoric strains are given by:

$$d\varepsilon_v^e = \frac{dp'}{K_{ref}\left(\frac{p'}{p'_{ref}}\right)^n} \quad \text{and} \quad d\varepsilon_d^e = \frac{dq}{3G_{ref}\left(\frac{p'}{p'_{ref}}\right)^n} \qquad (2)$$

Where K_{ref}, G_{ref} and n^e are, respectively, the bulk elastic modulus at a reference mean stress p'_{ref}, the reference shear elastic modulus at p'_{ref}, and the non-linearity exponent.

Plasticity is characterised by two different yield criteria, the isotropic yield function f_{iso} with an associated flow rule and the deviatoric yield function f_{dev} with a non-associative flow rule, each of which corresponds to a plastic mechanism associated to either the volumetric or distortional deformation mode (Equations 3a, 3b):

$$f_{iso} = p' - p'_c \cdot r_{iso} = 0 \qquad (3a)$$

$$f_{dev} = q - Mp'\left(1 - b\ln\frac{d \cdot p'}{p'_c}\right) \cdot r_{dev} = 0 \qquad (3b)$$

Where p'_c is the preconsolidation mean effective stress, b is a soil parameter which defines the shape of the deviatoric yield function, $d = p'_c / p'_{cr}$ is the ratio between the preconsolidation pressure p'_c and the corresponding critical state pressure p'_{cr}, r_{iso} and r_{dev} are internal hardening variables and M is the slope of the critical state line in plane $p' - q$. The formulation proposed by Van Eekelen (1980) is adopted to account for the third stress invariant Lode angle as shown below [16]:

$$M = 3\sqrt{3}\cdot\alpha_L\left(1+b_L\cdot\sin\left(3\vartheta\right)\right)^{nL} \quad (4)$$

Where ϑ is the Lode angle and a_L, b_L and n_L are material parameters. The plastic potential is given by [17]:

$$g_{dev} = q - \frac{\alpha}{\alpha-1}Mp'\left[1-\frac{1}{\alpha}\left(\frac{d\ p'}{p'_c}\right)^{\alpha-1}\right] \quad (5)$$

Where α is a soil parameter. The ACMEG-s model uses an isotropic hardening rule. The size of the elastic domain is controlled by the (apparent) preconsolidation pressure [18]:

$$p'_c = p'_{c0}\exp\left(\beta\varepsilon_v^p\right) \quad (6)$$

Where β is the plastic stiffness coefficient. The volumetric plastic strain ε_v^p is the internal hardening variable for both plastic mechanisms.
The ACMEG-s model presents a bounding surface plasticity formulation [19, 20].
The dependency of apparent preconsolidation pressure on matric suction is given by:

$$p'_c = \begin{cases} p'_{c0} & if \quad s \le s_E \\ p'_c = p'_{c0}\left\{1+\gamma_s\left[log\left(\frac{s}{s_E}\right)\right]^{n_{LC}}\right\} & if \quad s \ge s_E \end{cases} \quad (7)$$

Where p'_{c0} is the preconsolidation pressure at zero suction and reference void ratio e_{ref}, γ_s is a material parameter and s_E is the air entry suction. The apparent preconsolidation pressure remains constant up to the air entry suction since capillary effects only occur as air enters into the pore space and inter-particle menisci start to form.
Experimental data on the volcanic ashes suggest marginal hysteretic effects and dependency on void ratio [9]. In this sense, a Van Genuchten type soil water retention curve [21] is used in this analysis:

$$S_r = S_{res} + \frac{1-S_{res}}{\left[1+(\alpha s)^n\right]^m} \quad (8)$$

Ferrari et al. (2013) showed a clear dependency for a volcanic ash of the permeability on degree of saturation and void ratio. To account for that, the intrinsic isotropic permeability k_w^{int} is expressed as a function of initial void ratio e_0 and volumetric strain ε_v:

$$k_w^{\text{int}} = k_w^{\text{int},0}\left[e_0 - \varepsilon_v\left(1+e_0\right)\right]^{c_k} \quad (9)$$

where $k_w^{int,0}$ is the intrinsic isotropic permeability for a reference void ratio $e_{ref} = 1$ and the exponent c_k is a fitting parameter.
All the constitutive models parameters for the volcanic ash involved in this study were obtained through extensive laboratory tests [9, 22]. The ACMEG-s model and the soil water retention model are implemented into the nonlinear finite element code LAGAMINE which solves mass balance equation and the momentum equation [23, 24].

The finite element model

Hydro-mechanically coupled slope simulation is run for a two-dimensional slope section in plain strain conditions, representing the steepest slope section above a Pozzolana quarry on the South-West slope of Irazu Volcano at 2'500 m above sea level (Figure 1). The finite element model is built on the basis of topographical data of the landslide-prone area situated above the quarry. The volcanic ash mantling the consistent and relatively impermeable Pozzolana bedrock is assumed to present generally a constant thickness of 3 m. The volcanic ash is characterised as fairly homogeneous, cohesionless silty sand with a shearing resistance angle $\phi' = 35.5°$. The natural water content is in the range of 0.22-0.24 and the average dry unit weight $\gamma_d = 9.9$ kN/m^3, which yields an average void ratio of 1.58 [9].
The soil cover is separated into two material layers with preconsolidation pressure increasing from the top to the bottom layer aiming at reproducing normally consolidated conditions prior to rain infiltration. The Pozzolana bedrock is modelled as an elastic, impermeable body. Uniform matric suctions equal to 20 kPa are defined in the slope as initial conditions. After an initial gravity initialisation phase, a hydro-mechanical simulation is run over a period of 64 days of the wet season of 2005.
Hydro-mechanically coupled simulations were run in order to analyse the slope response to realistic rainfall scenarios, with the aim to gather information on the evolution of significant geomechanical variables such as matric suction, volumetric and deviatoric deformations. Real rainfall conditions are simulated here on the basis of daily rainfall data from Juan Santamaria Int. airport close to the capital San José (NOAA 2011) [25].

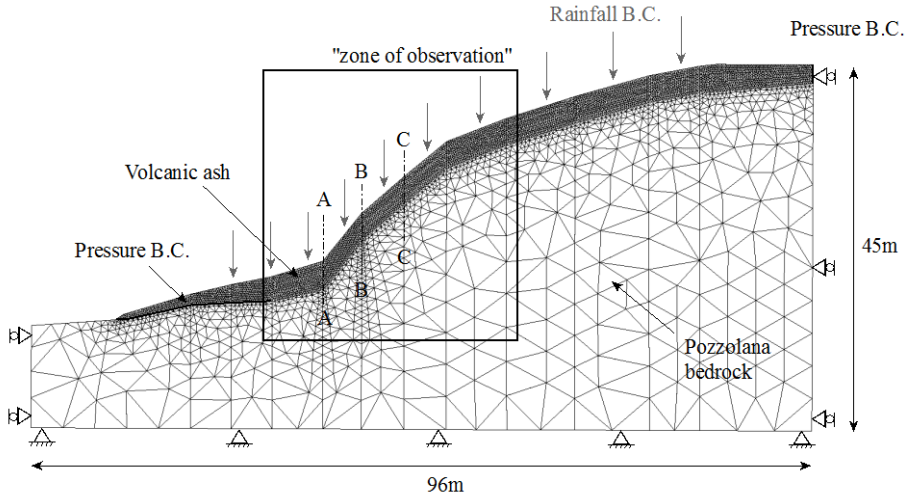

Figure 1. Two-dimensional slope section, representing the steepest slope section above a Pozzolana quarry on the South-West slope of Irazu Volcano at 2'500 m above sea level.

Selected results and process understanding

As an example of the outcomes of the modelling results, the evolution in time of matric suction is plotted in Figures 4a and for the vertical section A, indicated in Figure 2. Matric suctions within the first meter of soil depth fluctuate in accordance with daily rainfall input. At the toe of the slope, the suction response is more progressive as a consequence of lateral subsurface flow moving water from the top to the bottom of the slope. Between 2 and 3 m soil depth, matric suctions remain low even during longer dry periods (e.g. day 25-35). In the 0.5

m above the bedrock, suctions are monotonically decreasing, which is an indicator for worsening slope stability conditions throughout the wet season. This indicates also the presence of continuous, lateral groundwater flow in the quasi-saturated zone above the impermeable substratum. As a consequence of variable rainfall boundary conditions and the complex unsaturated hillslope flow regime, the volcanic ash undergoes stress paths involving cyclic changes in effective stresses. The capillary stress changes lead together with total stress changes from rain infiltration and stress redistributions within the slope to cyclic variations in mean effective stresses and deformations. Volumetric plastic strains occur primarily in locations with strong losses in matric suctions due to the normally consolidated state of the volcanic ashes. The temporal evolution of volumetric plastic strains is displayed for section B and three different depths (1, 2 and 3 m) in Figure 3. Noticeable increases in contractive volumetric strains are observed after 15, resp. 39 days, both of which correspond to series of 3 to 4 days of consecutive rainfall.

The deviatoric plastic strain contours indicate for the steep part of the slope section shear localisation along the interface between bedrock and soil cover. Based on the distinctive magnitude of plastic deviatoric strains in the lower part of the slope towards the surface, it can be stated that the most probable failure mechanism would surface at the toe of the slope. The location of the bedrock has clearly a strong influence on the probable failure mechanism. In analogy to the volumetric behaviour, plastic deviatoric strains increase significantly after particularly rainy periods. Deviatoric stresses undergo cyclic variations correlated to wetting and drying periods as shown in Figure 4.

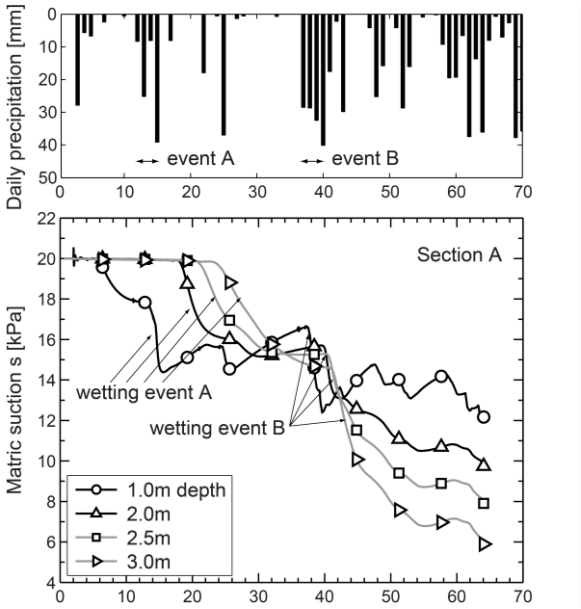

Figure 2. Evolution of matric suction at different depths for the vertical section (slope angle β=51°).

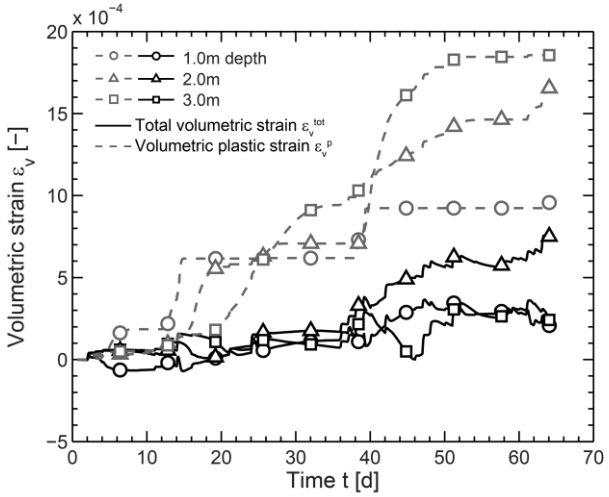

Figure 3. evolution of volumetric strains in section B

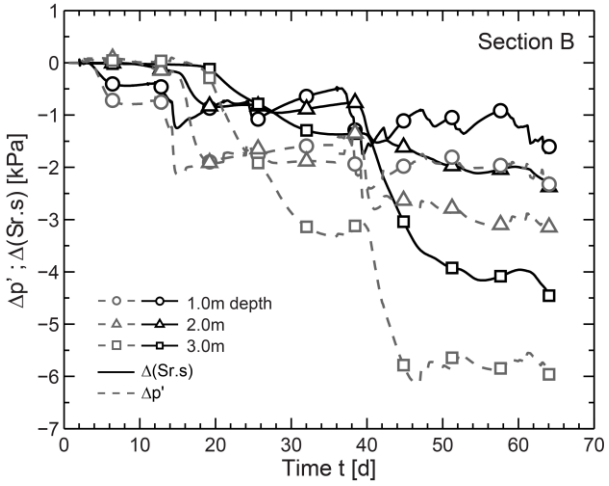

Figure 4. variations in mean effective stresses $\Delta \boldsymbol{p}' = \boldsymbol{p}' - \boldsymbol{p}'_{t=0}$ and capillary stresses $\Delta(\boldsymbol{S_r} \cdot \boldsymbol{s}) = (\boldsymbol{S_r} \cdot \boldsymbol{s}) - (\boldsymbol{S_r} \cdot \boldsymbol{s})_{t=0}$ at 1, 2 and 3 m of soil depth in section B.

Conclusions

A continuum modelling framework was presented for the analysis of instability processes at the onset of failure in loose volcanic ash slopes. Unlike slope stability methods representing failure with a single plastic limit condition, the bounding surface and multi-mechanism plasticity model with a hydro-mechanically coupled formulation is suitable for representing instability processes in unsaturated volcanic ash slopes subjected to rain infiltration.

The analysis of the results from the transient 2D slope simulation revealed the complex flow regime in the volcanic ash cover with unsaturated conditions. Wetting pore-collapse occurs in locations with strong losses in matric suctions and steep slope sections with strongly anisotropic stress states. Besides capillary stress changes, total stress changes from rain infiltration and stress redistributions were observed to influence the stress paths and the overall stability of the slope.

Acknowledgements

The following projects are acknowledge: SafeLand, "Living with landslide risk in Europe: Assessment, effects of global change, and risk management strategies," under Grant Agreement No. 226479, Wandland, "Effects of wetting and drying cycles on landslide activity," under Grant Agreement No. PERG06-GA-2009-256426 in the 7th Framework Programme of the European Commission, and TRAMM 2 "Swiss Competence Center Environment and Sustainability". The authors gratefully acknowledge Mr. James Fern for the rainfall data collection.

References

[1] Crosta G.B., Dal Negro P. Observations and modeling of soil slip-debris flow initiation processes in pyroclastic deposits: the Sarno 1998 event. *Natural Hazards and Earth System Sciences* (2003); 3: 53-69.
[2] Cascini L., Cuomo S., Guida D. Typical source areas of May 1998 flow-like mass movements in the Campania region, Southern Italy. *Engineering Geol*ogy (2008); 96: 107-25.
[3] Fuchu D., Lee C.F., Sijing W. Analysis of rainstorm-induced slide-debris flows on a natural terrain of Lantau Island, Hong Kong. *Engineering Geol*ogy (1999); 51: 279-90.
[4] Capra L., Lugo-Hubp J., Borselli L. Mass movements in tropical volcanic terrains: the case of Teziùtlan (Mexico). *Engineering Geol*ogy (2003); 69: 359-79.
[5] Crosta G.B., Imposimato S., Roddeman D., Chiesa S., Moia F. Small fast-moving flow-like landslides in volcanic deposits: The 2001 Las Colinas Landslide (El Salvador). *Engineering Geol*ogy (2005); 79: 185-214.
[6] Harp E.L., Reid M.E., McKenna J.P., Michael J.A. Mapping of hazard from rainfall-triggered landslides in developing countries: Examples from Honduras and Micronesia. *Engineering Geol*ogy (2009); 104: 295-311.
[7] U.S. Agency for International Development Fact Sheet #17, 1998.
[8] Picarelli L., Olivares L., Avolio B. Zoning for flowslide and debris flow in pyroclastic soils of Campania Region based on infinite slope analysis. *Engineering Geol*ogy (2008); 102: 132-41.
[9] Ferrari A., Eichenberger J. and Laloui L. Hydro-mechanical behaviour of a volcanic ash. *Geotechnique* (2013); 63(11): 1433-1446.
[10] Nuth M. Constitutive modelling of unsaturated soils with hydro-geomechanical couplings. Ecole Polytechnique Fédérale de Lausanne, Switzerland. Ph.D. thesis (2009).
[11] Nuth M., Laloui L. New insight into the unified hydro-mechanical constitutive modelling of unsaturated soils. Unsat Asia, Nanjing (2007); 109-125.
[12] Nuth M., Laloui L. Advances in modelling hysteretic water retention curve in deformable soils. *Computers and Geotechnics* (2008); 35(6): 835-844.
[13] Salager S., Nuth M, Ferrari A, Laloui L. Investigation into water retention behaviour of deformable soils. *Canadian Geotechnical Journal* (2013); 50(2): 200-208.
[14] Nuth M., Laloui L. Effective stress concept in unsaturated soils: Clarification and validation of a unified framework. *International Journal for Numerical and Analytical Methods in Geomechanics* (2008); 32: 771-801.
[15] Laloui L., Nuth M. On the use of the generalised effective stress in the constitutive modelling of unsaturated soils. *Computers and Geotechnics* (2009); 36: 20-23.
[16] Di Donna, A., Laloui L. Numerical analysis of the geotechnical behaviour of energy piles. *International Journal for Numerical and Analytical Methods in Geomechanics* (2014). DOI: 10.1002/nag.2341.
[17] Nova, R. & Wood, D.M. A constitutive model for sand in triaxial compression. *International Journal for Numerical and Analytical Methods in Geomechanics* (1979); 3: 225-278.
[18] Hujeux J. Une loi de comportement pour le chargement cyclique des sols. Génie Parasismique. Paris, Les édition de l'E.N.P.C. (1985) ; 287-353.
[19] Hujeux J. Calcul numérique de problèmes de consolidation élastoplastique. Ecole Centrale Paris, France. Ph.D. thesis (1979).
[20] Dafalias Y., Hermann L. A bounding surface soil plasticity model. International Symposium on Soils under Cyclic and Transient Loading, Swansea (1980); 335-45.
[21] Van Genuchten M.Th. A closed-form equation for predicting the hydraulic conductivity of unsaturated soil. *Soil Science Society of America Journal* (1980); 44(5): 892-898.
[22] Ferrari A., Eichenberger J., Fern J., Ebeling P.and Laloui L. Experimental and numerical analysis of an unsaturated volcanic ash deposit for the establishment of an early warning system in a quarry in Costa Rica. Geocongress 2012: State of the Art and Practice in Geotechnical Engineering, Oakland, Geotechnical Special Publications No. 225. ASCE, 2012, 2512-2521.
[23] Charlier R. Approche unifiée de quelques problèmes non linéaires de mécanique des milieux continus par la méthode des éléments finis. University of Liège, Belgium. Ph.D. thesis (1987).
[24] Collin F. Couplages thermo-hydro-mécaniques dans les sols et les roches tendres partiellement saturés. University of Liège, Belgium. Ph.D. thesis (2003).
[25] Eichenberger J., Ferrari A., Laloui L. Early warning thresholds for partially saturated slopes in volcanic ashes. *Computers and Geotechnics* (2012); 49, 79-89.

Contrasting landslide movement rates – geological influences and engineering behaviour

Fred Baynes

Past President of IAEG, Malmsbury, Australia

The first landslide is a slow moving suburban landslide in Australia. Figure 1 is a photo of the area. The landslide is developed in Tertiary slope deposits adjacent to an inactive fault scarp (Figure 2). During the development of housing in the area the presence of the old degraded landslide was not recognised and the poorly built subdivision resulted in increases in infiltration from leaking services, excessive garden watering and in one case a badly leaking swimming pool. This started a cycle of slight movements, rupture of services, leakage of water rises of groundwater levels and further movements.

Figure 1 View of Landslide1

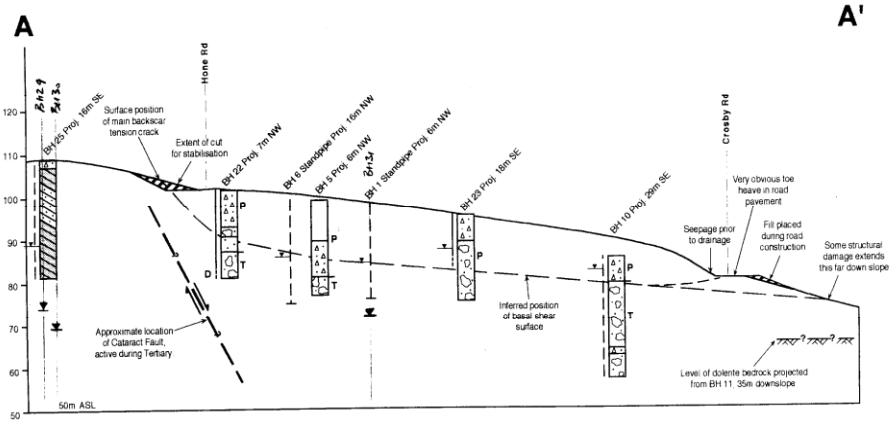

Figure 2 Cross section of Landslide1

The landslide movements were stopped by drainage from both horizontal drains and vertical bores with pumps in early 1990. The landslide was then monitored for 25 years. The stabilization was effective apart from a period when the pumps were switched off and this action, together with leaking services, combined to increase groundwater levels and some slight movements developed (Figure 3).

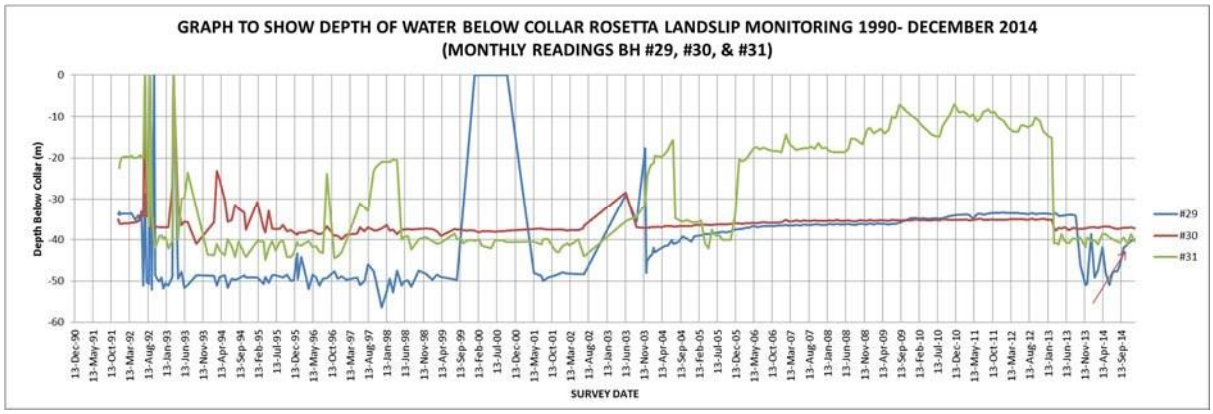

Figure 3 Piezometric levels in Landslide1

This was a relatively simple well understood landslide that has behaved in a predictable manner.

Figure 4 Photo of Landslide 2

The second landslide is a 15 million cubic metre slow moving landslide that developed within a geothermally active volcanic crater in Papua New Guinea (Figure 4). The crater hosts an open cut gold mine and the mining activity cause movement of a pre-exiting landslide. However the landslide suddenly and unexpectedly accelerated to 20 km/hr, developed two lateral mudflows, initiated a tsunami, killed two people and completely disrupted the mine operation. A very detailed geological model of the landslide and surrounds was developed to engineer a mine expansion, numerous sections through the landslide were developed and one is presented as Figure 5 to illustrate the geological complexity and the possible effects of geothermal flux beneath the landslide.

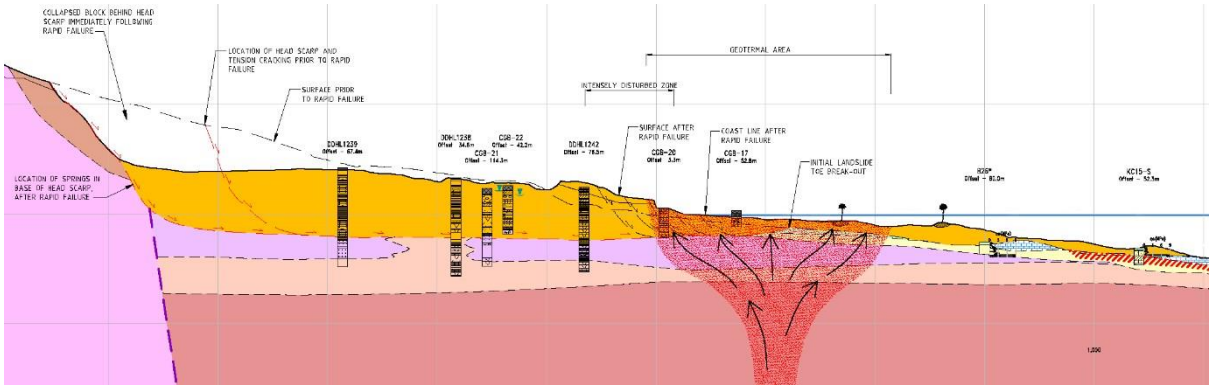

Figure 5 Cross section through landslide 2

The movements of the landslide over the 12 months prior to the catastrophic failure are indicated in Figure 6. The reasons for the sudden acceleration may be due to increased water inflows into the rear of the slope, blocking of geothermal vents or a geothermal outburst or some changes to the soil strength that took place in this complex geological environment, or a combination of these factors.

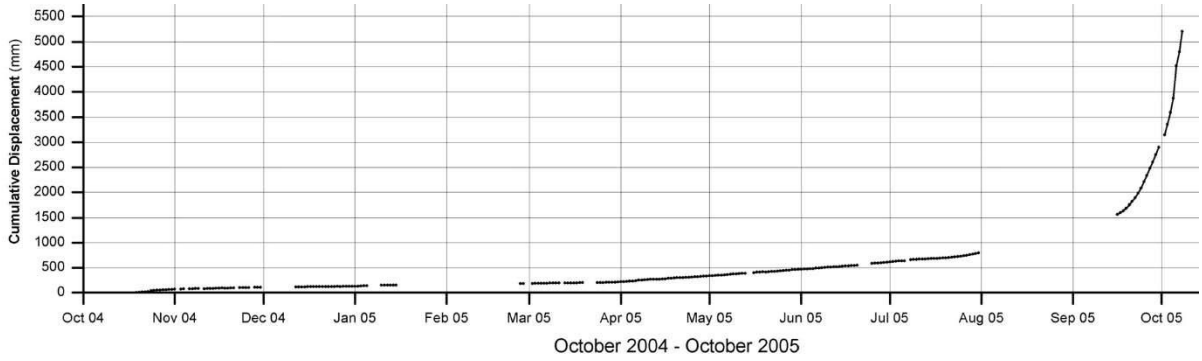

Figure 6 Movement record Landslide 2

This was a poorly understood landslide in a complex geological environment with active surface processes and the landslide behaved in an unpredictable manner and represents an ongoing engineering challenge.

Climate impacts on slopes

D. G. Toll

School of Engineering and Computing Sciences, Durham University, Durham, UK

The research project iSMART (Infrastructure Slopes: Sustainable Management And Resilience Assessment) is a collaboration between six UK academic partners (University of Newcastle upon Tyne; Durham University; University of Loughborough; University of Southampton; Queen's University Belfast and the British Geological Survey) and 11 asset owners and industrial partners. Together, the partners are using a combination of field measurements, laboratory testing and development of conceptual and numerical models to improve our understanding of the interaction between weather, vegetation and soil. This understanding is aimed at helping managers of the UK's transport infrastructure to identify problem sites, plan and prioritise maintenance activity, and develop design, assessment and adaptation strategies to ensure the future safety and resilience of geotechnical transport infrastructure.

The UK's transport infrastructure is one of the most heavily used in the world. The performance of the transportation networks is critically dependent on the performance of cutting and embankment slopes. Many of these slopes are old and suffering high incidents of instability (increasing with time). There is evidence that the scenario of increased (and more intense) rainfall has already had an impact on UK transport infrastructure (Kilsby et al., 2009) and climate change scenarios for the UK present the potential for these issues to accelerate.

One of the sites being monitored within the iSmart project is an instrumented embankment to investigate the response to changing climatic conditions. The BIONICS embankment was built at Nafferton farm in North East England and construction was completed in November 2005 (Hughes et al., 2009). The embankment dimensions are 90 m long by 6 m high with side slopes of 1 in 2 (V:H) and a 5 m width crest. The BIONICS embankment has been equipped with a system of sprinklers and covers to control climatic conditions. It has been fully instrumented with piezometers, tensiometers, water content and temperature sensors, inclinometers and extensometers. The experimental facility provides essential field measurements that can be used to calibrate numerical models of soil responses to climatic changes.

The fill material used to build the BIONICS embankment was a glacial till (Durham Lower Boulder Clay), a common fill material in North East England and hence representative of earthwork construction. The fill material can be classified as a sandy clay of intermediate plasticity.

As an experimental embankment the BIONICS embankment was intended to be used as a platform for new testing methodologies that can help the investigation and determination of soil behaviour. A novel experimental set-up for field monitoring of soil suctions was developed for the BIONICS embankment (Mendes et al., 2008; Toll et al., 2011). The experimental set-up used Durham University high capacity tensiometers (Lourenço et al., 2006; Toll et al., 2013) to provide real-time continuous measurements of suction inside the embankment. The wide measuring range of the tensiometers (suction of 2 MPa) allows the monitoring system to be used in most natural and constructed earth structures.

The results of monitoring in Figure 1 show the cycles of pore water pressure that might be expected in an embankment in the UK (Toll et al., 2012). Results within the core of the embankment show higher pore water pressures (near to hydrostatic) were observed during

winter months (typically January) falling back to lower values in March. Lower values might normally be expected during summer months, but the climate during the summers of 2007, 2008 and 2012 were "untypical" with high levels of summer rainfall, as well as being subject to artificial inundation.

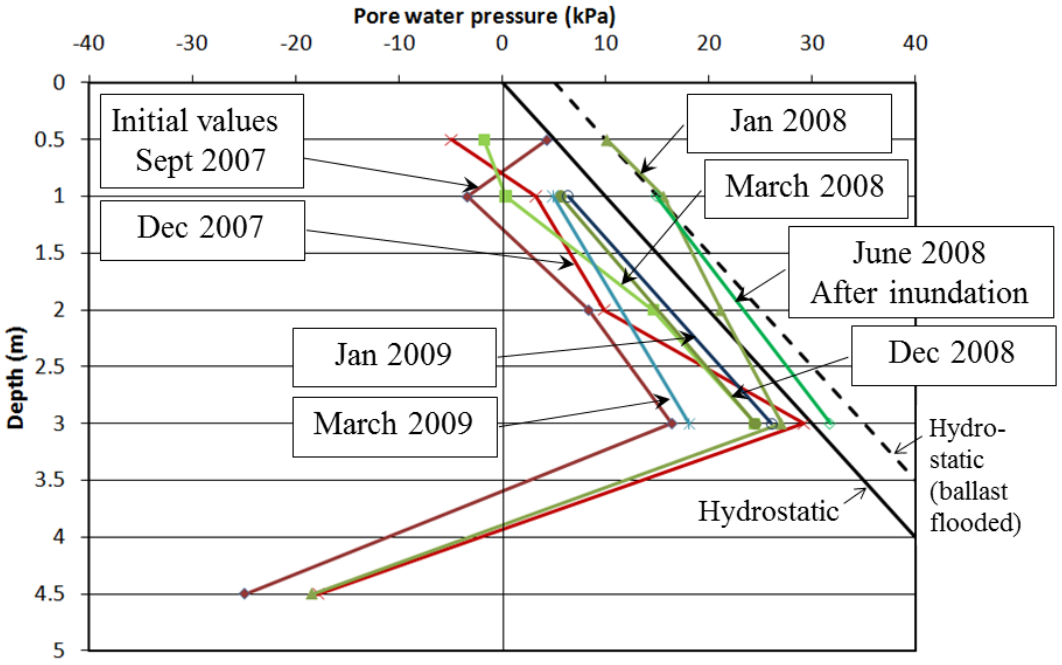

Figure 1. Pore water pressure profiles measured in the core of the BIONICS embankment

Results of suction monitoring of the slope faces by University of Newcastle upon Tyne show suctions of the order of 500-600kPa being generated near to the surface (0.5m) during drier period (R. Stirling, Pers. Comm.). In some years, two drier periods were observed during the summer months separated by a wetter period in August. During the wet summer of 2012, no dry period was observed.

The British Geological Survey have installed Electrical Resistance Tomography arrays on the embankment that allows water content profiles to be monitored with time. Laboratory investigations have been carried out at Durham and Newcastle upon Tyne universities to provide calibrations to relate water content and electrical resistivity for the BIONICS soil.

Some of the findings of the project so far are:

- Changes in climate are already having an effect on transport infrastructure in the UK. Climate models suggest that the extremes of wetting and drying will increase.
- High suction tensiometers have been used to monitor pore pressure changes in response to climate events for an instrumented embankment (BIONICS).
- In storm events, pore water pressures can approach hydrostatic conditions in the upper 3m.

- In the dry season, high suctions (500-600 kPa) can develop on the upper surface of the side slopes.
- Electrical Resistivity Tomography can provide water content cross-sections within embankments over time.

References

Hughes, P.N., Glendinning, S., Mendes, J., Parkin, G., Toll, D.G., Gallipoli, D. and Miller, P. (2009). Full-scale testing to assess climate effects on embankments. Special Issue of Engineering Sustainability, Institution of Civil Engineers, 162, No. ES2, pp. 67-79.

Kilsby, C., Glendinning, S., Hughes, P. N., Parkin, G. and Bransby, M. F. (2009) *Climate-change impacts on long-term performance of slopes*, Proc. Institution of Civil Engineers - Engineering Sustainability 162, pp. 59–66.

Lourenço S.D.N., Gallipoli, D., Toll, D.G. and Evans, F.D. (2006) *Development of a commercial tensiometer for triaxial testing of unsaturated soils*, Geotechnical Special Publication No. 147, Reston: American Society of Civil Engineers, Vol. 2, 1875-1886.

Mendes, J., Toll, D.G., Augarde, C.E. and Gallipoli, D. (2008) *A System for Field Measurement of Suction using High Capacity Tensiometers*, Unsaturated Soils: Advances in Geo-Engineering (eds. Toll, D.G., Augarde, C.E., Gallipoli, D., Wheeler, S.J.), Leiden: CRC Press/Balkema, pp. 219-225.

Toll, D.G., Lourenço, S.D.N. and Mendes, J. (2013) Advances in suction measurements using high suction tensiometers, Engineering Geology, Vol. 165, pp 29–37.

Toll, D.G., Lourenço, S.D.N., Mendes, J., Gallipoli, D., Evans, F.D., Augarde, C.E., Cui, Y.J., Tang, A.M., Rojas, J.C., Pagano, L., Mancuso, C., Zingariello, C., Tarantino, A. (2011) *Soil Suction Monitoring for Landslides and Slopes*. Quarterly Journal of Engineering Geology and Hydrogeology, 44(1), pp. 23-33.

Toll, D.G., Mendes, J., Gallipoli, D., Glendinning, S. and Hughes, P.N. (2012) *Investigating the Impacts of Climate Change on Slopes: Field Measurements*, in Earthworks in Europe, Geological Society of London, Special Publication Vol. 26, pp. 151-161.

D8 motorway Dobkovičky landslide: the case history and repair options

Petr Kycl
Czech Geological Survey, Czech Republic

The plans for a highway connecting Prague with Dresden have been debated since 1930´s. The German engineers planned "Autobahn A72" already in 1938. Construction of the first 4.2 km of totally 92 km long D8 motorway began in the section 0806 Řehlovice – Ústí nad Labem nearly 50 years later in 1984. The construction of the last remaining 16.2 km in the section 0805 Lovosice – Řehlovice was launched in 2007. This section crossed České středohoří Mts. which represents geologically most complex and problematic part for the motorway, in particular due to the presence of large area of dormant and abandoned landslides know as "Prackovice landslides" intersected by the motorway.
On Friday, June 7th 2013, the works were interrupted and the motorway under construction was damaged when heavy rains triggered a landslide near village Dobkovičky (km 56.3–56.5: fig. 1).


Fig. 1: Damaged motorway D8 which was under construction at the time of landslide.

The damage was not restricted only to the motorway (fig. 1) but also affected the single-track railway Lovosice – Teplice between the stations Dobkovičky and Radejčín (fig. 2). The railway was completely destroyed in the length of 200 m, including a 6 m high embankment.

Fig. 2: Destroyed railway.

Fig. 3: Damages in the Dobkovičky quarry.

Site investigation

The site investigations of the landslide lasting for two months and carried out by the AZ Consult Company began at the end of April 2014 (fig. 4). The survey comprised 15 boreholes (of which 4 were inclinometric, 6 hydro-geological and 5 engineering geological) complemented with 2 dug holes and 7 geophysical profiles. The aims of the investigations were to determine surface of rupture (fig. 5), geotechnical properties of the soils and rocks necessary for the stability calculating, effect of the superficial and underground water and finally to create the geotechnical model of the landslide.

Fig. 4: Site investigation – borehole HV103.

Fig. 5: Surface of rupture in dug hole KS-1.

Remediation – I. phase

Finally, the remediation works started on November 18th 2014. The first phase comprised excavation of 80.000 m^3 of the slid masses from the upper part of the landslide. At the same time, superficial drainage channel has been realized. When measurements confirm the landslide is stable, the II. phase can be approached.

Fig. 6: Excavation of 80.000 m^3 in the upper part.

Fig. 7: Final form of landslide in the upper part.

The tender for the project of the II. phase has been actually announced. The II. phase will include deep drainage and static elements in the line above the motorway. The static elements will be probably based on the underground piles or wall segments ("T elements"). The start of the II. phase is expected for the turn 2015/16. Finally the landslide accumulation from the motorway can be excavated, and reconstruction of the asphalt surface and drainage of highway will follow. December 2016 is the actual deadline for opening of the D8 motorway.

23TH PRAGUE GEOTECHNICAL LECTURE

A Particle Level Review of Soil Behavior and Macroscale Implications

J. Carlos Santamarina

King Abdullah University of Science and Technology **(**KAUST**),** Saudi Arabia

Soils are made of grains. Particle size and shape reflect material composition, formation history, transportation, and depositional environment. Prevalent formation processes for small and large mineral grains include: mechano-genesis (silts and sands - Nominal size d>10μm; from angular to rounded), chemo-genesis: from solution (e.g., clay minerals - Nominal size <10μm; platy, tubular, spherical), biogenesis (microfossils such as diatoms - Nominal size d~5-to-100μm; intricate shape and internal pore structure), and thermogenesis: from melt (Ash - Nominal size: 1μm to 1mm; from xenospheres to shards). Specific surface is determined by the smallest particle dimension and is intimately linked to the relevance of surface related processes.

Soils are not inert. Changes within engineering time scales can have a profound effect on their physical properties. Structural (e.g., compaction, crushing), chemical (e.g., dissolution and precipitation) and bio-mediated processes (including clogging and biogass) alter the stress field, can govern stiffness, and can play a crucial effect in fluid conductivity and pore pressure generation. As a corollary, natural soils may behave differently than freshly remolded clay or recently packed sand.

Soil deformation implies particle-level forces. Forces can be generated at the boundary and transmitted through the granular skeleton (i.e., due to effective stress), result from the particle volume (weight and buoyancy), develop along the particle surface (hydrodynamic and capillary) and/or arise at the contact (electrical and cementation-reactive). These forces scale with: d^3 (weight and buoyancy), d^2 (skeletal), d^1 (hydrodynamic, capillary and electrical), or are independent of particle size i.e., d^0 (cementation - reactive). Capillary forces start being relevant to soil behavior for grains smaller than ~100μm. van der Waals attraction controls aggregation during sedimentation and the mobilization of fines in pores during seepage. Electrical repulsion gains relevance in high specific surface clays S_s at low void ratio so that the interparticle separation is small.

The sieve #200. The analysis of particle size, shape and governing interparticle forces shows (1) a marked distinction in grain formation mechanisms across the 10μm-to-100μm grain size divider, (2) the increased significance of capillary forces for grains smaller than sieve #200, and of electrical forces for grains smaller than 1-to-10μm. Clearly, the sieve #200 is an excellent choice to discriminate between coarse and fine grained soils.

Fine grained sediments exhibit pore fluid chemistry-dependent fabric and behavior. This property is of critical relevance to frequent field conditions that involve hydro-chemo-mechanical coupled process. The liquid limit measures not only water adsorbed onto particle surfaces, but also held in the pore space of the fluid-dependent fabric. Therefore, fluid

chemistry-dependent inter-particle interactions can be probed by running liquid limit tests on pastes prepared with fluids of contrasting permittivity and electrical conductivity. Liquid limits determined with deionized water, NaCl brine and kerosene are combined to capture "soil plasticity" and "electrical sensitivity" S_E. Together, these two measurements can effectively discriminate fine-grained soils according to their response to pore fluids and lead to their enhance classification.

Coarse grained sediment behavior is determined by grain size distribution and particle shape (readily confirmed by experimental trends for packing densities e_{min} and e_{max}). In gap-graded mixtures, two values can be computed for the fines content when the finer fraction fills the voids between coarse particles: (1) *low fines fraction* threshold when coarse grains are densely packed and the fine component is loosely packed, and (2) *high fines fraction* threshold when coarse grains are loosely packed and the fine component is densely packed. Hydraulic conductivity stiffness, strength, minimum and maximum packing densities, and dilative tendencies are intimately related to fines fraction in relation to the low and high fraction thresholds. Soil classification systems must be augmented to properly recognize grain shape, size distribution and mixture thresholds.

Pore size and pore connectivity determine hydraulic conductivity, the evolution of mixed-fluid conditions (unsaturated soils, soil water characteristic curve), and geometric limits for bioactivity. Geometrical analyses show that pore size is intimately related to grain size. The mean pore size can be estimated as a function of void ratio and specific surface. Published pore size distribution data for clays, silts, and sands show that the standard deviation of $\ln(d_p/[\mu m])$ is around 0.4.

Hydraulic conductivity. Compiled experimental data confirms that hydraulic conductivity is strongly determined by void ratio and specific surface, even in the absence of pore network information. Given a hydraulic conductivity k_o for a soil at void ratio e_o, the hydraulic conductivity k as the soil compresses to void ratio e can be estimated as $k/k_o=(e/e_o)^n$, where the exponent is $n\approx3$ for coarse grained soils and $n\approx4$ for fine grained soils. A relatively small fraction of pores is responsible for most of the flow; this has important implications to the evolution of dissolution in reactive fluid flow.

From small to large strains. Particle-level deformation mechanisms change with strain level. Small-strain deformation takes place at constant-fabric and grain deformations concentrate at inter-particle contacts; in this strain regime, volume change, pore pressure generation and frictional losses are minimal. Large-strain deformation involves fabric changes and the role of contact-level grain deformation vanishes. The threshold strain between the two regimes is higher for smaller particles and at higher confinement.

Small-strain stiffness. The small strain stiffness in remolded specimens is determined by the state of stress. On the other hand, the stiffness of diagenetically modified, aged sediments can be significantly higher due to contact stiffening (creep, cementation, pressure solution-precipitation). Sampling and distressing can have a pronounced effect on stiffness. The small strain stiffness can be readily measured in the laboratory and in the field, and it is most valuable for deformation analyses.

Compressibility. Different processes are responsible for the void ratio at low, intermediate and high stress. Soil compressibility models with physically correct asymptotic values are required to analyze situations that involve a wide stress range. The classical e-log(σ) function,

as well as power, exponential, hyperbolic, and arctangent functions, can be adapted to satisfy asymptotic void ratios at low and high stress levels. All updated models involve 4 physically meaningful parameters and can adequately fit remolded soil compression data for a wide range of stresses and soil types. Models that involve the power of the stress σ'^{β} display higher flexibility to capture the brittle response of some structured natural sediments with a sharp brittle transition at the yield stress. The use of a single continuous function to capture soil compressibility data avoids numerical discontinuities or the need for ad hoc procedures to determine the yield stress.

Shear strength combines dilation and constant volume friction. Dilation depends on packing density (function of grain size distribution, mixture fraction and particle shape), applied confinement and cementation. Constant volume friction is determined by particle geometry, both in fine and coarse-grained sediments.